MMP-9 Reinforces Radiation-Induced Delayed Invasion and Metastasis of Surviving Neuroblastoma Cells Through Second-Signaling Positive Feedback With NFkB Via Both ERK and IKK Activation

Dinesh Babu Somasundaram
The University of Oklahoma Health Sciences Center
Sheeja Aravindan
The University of Oklahoma Stephenson Cancer Center
Ryan Major
The University of Oklahoma Health Sciences Center
Mohan Natarajan
The University of Texas Health Science Center at San Antonio
Natarajan Aravindan (naravind@ouhsc.edu)
The University of Oklahoma Health Sciences Center https://orcid.org/0000-0001-9150-3911

Research Article

Keywords: progressive neuroblastoma, NFkB, MMP9, therapy pressure, radiation therapy

Posted Date: March 22nd, 2021

DOI: https://doi.org/10.21203/rs.3.rs-311771/v1

Abstract

Neuroblastoma (NB) progression is branded with hematogenous metastasis and frequent relapses. Despite intensive multimodal clinical therapy, outcomes for patients with progressive disease remain poor, with negligible long-term survival. Therefore, understanding the acquired molecular rearrangements in surviving cells with therapy pressure and developing improved therapeutic strategies is a critical need to improve the outcomes for high-risk NB patients. We investigated the rearrangement of MMP9 in NB with therapy pressure, and unveiled the signaling that facilitates NB evolution. Radiation-therapy (RT) significantly increased MMP9 expression/activity, and the induced enzyme activity was persistently maintained across NB cell lines. Further, RT-triggered NFkB transcriptional activity and this RT-induced NFkB were required/adequate for MMP9 maintenance. RT-triggered NFkB-dependent MMP9 actuated a second-signaling feedback to NFkB, facilitating a NFkB-MMP9-NFkB positive feedback cycle (PFC). Critically, MMP9-NFkB feedback is mediated by MMP9-dependent activation of IKKβ and ERK phosphotransferase activity. Beyond its tumor invasion/metastasis function, PFC-dependent MMP9 lessens RT-induced apoptosis and favors survival pathway through the activation of NFkB signaling. In addition, PFC-dependent MMP9 regulates 19 critical molecular determinants that play a pivotal role in tumor evolution. Interestingly, seven of 19 genes possess NFkB-binding sites, demonstrating that MMP9 regulates these molecules by activating NFkB. Collectively, these data suggest that RT-triggered NFkB-dependent MMP9 actuates feedback to NFkB though IKKβ- and ERK1/2-dependent IkBα phosphorylation. This RT-triggered PFC prompts MMP9-dependent survival advantage, tumor growth, and dissemination. Targeting therapy-pressure-driven PFC and/or selective inhibition of MMP9 maintenance could serve as promising therapeutic strategies for treatment of progressive NB that defies current clinical therapy.

Introduction

Matrix metalloproteinase (MMPs) are zinc-containing endopeptidases that degrade extracellular matrix (ECM) machinery (Klein, Bischoff 2011). Constitutively, MMPs reside as latent zymogens that become active through multiple mechanisms (e.g., cysteine, allosteric, furin, MMPs, plasmin)(Ra, Parks 2007) and prompt the degradation of matrix barriers. Programmed remodeling of ECM is a key step in cancer evolution, and the MMP-dependent degradation of matrix barrier is critical for tumor cell migration, invasion, and metastasis (Stetler-Stevenson 1990). High expression levels and enzyme activity of MMPs are evident in in malignant tumors, compared with normal, benign, or even in premalignant tissues (Sternlicht, Werb 2001). Functionally, MMPs are involved in tumor cell proliferation (by release of growth factors [GF], cleaving GF-binding proteins and GF-receptors); invasion (by generating an α1-antitrypsin cleavage product); epithelial to mesenchymal transition (EMT); angiogenesis (release of angiogenesis factors); cell cycle checkpoint control; genomic instability; and clonal selection (anchorage-independent and apoptosis-resistant) (Lukashev, Werb 1998; Suzuki et al. 1997; Fowlkes et al. 1994; Levi et al. 1996; Kataoka et al. 1999; Tlsty 1998; Thomasset et al. 1998; Sternlicht et al. 2000). The function of MMPs in altering the metastatic state of cancer cells and the association of MMPs expression with poor prognosis has been recognized in different cancers, including neuroblastoma (NB)(Chavali et al. 2014; Sugiura et al.

1998; Ara et al. 1998). In particular, MMP-9, a 92kDa type IV collagenase that plays a vital role in cancer cell invasion and metastasis, is well characterized (Kalavska et al. 2021). However, the function of MMP9 in NB evolution, particularly its reinforcement under therapeutic pressure and the signaling involved, is thus far unrealized.

Neuroblastoma, the most aggressive extra-cranial solid tumor occurring in childhood, remains a major cause of cancer death in infancy (Matthay et al. 2016). Clinically, neuroblastoma progression is branded with hematogenous metastasis and frequent relapses, with a rapidly decreasing timeline (Santana et al. 2008). Despite the current intensive and multimodal therapeutic strategies (chemotherapy, radiotherapy, surgery, immunotherapy, stem cell transplant, 13-cisretinoic acid), outcomes for progressive heterogeneous disease remain poor, with negligible long-term survival (London et al. 2011). Therefore, unveiling the acquired molecular rearrangements in response to current clinical therapy and developing new therapeutic strategies are critical to improve the clinical outcomes for NB patients. Radiation therapy (RT) is one of the mainstream treatment modalities for NB treatment and provides many benefits, such as: shrinking tumors prior to surgery to enable ease of surgery; treating larger tumors that affect breathing; treating tumors that do not respond quickly to chemotherapy; destroying leftover NB cells after stem cell transplant for high-risk disease; and relieving pain caused by advanced disease. Ultimately, the goal of RT is to kill as many cancer cells as possible while limiting harm to nearby healthy tissue. Conversely, RT-induced radioresistance in cancer cells is a fundamental barrier limiting the effectiveness of RT. We provided first evidence on the existence of radioresistance in NB cells after clinically relevant fractionated RT (Madhusoodhanan et al. 2009; Veeraraghavan et al. 2011). Further, we unveiled the intercellular molecular cross talk and the signaling mechanisms involved in NB cell radioresistance (Aravindan et al. 2011; Veeraraghavan et al. 2011; Aravindan et al. 2014). It is pertinent to understand how this RT-induced signaling translates into cellular function that contributes to NB evolution.

MMP-9 protein contains five domains (hemopexin-like, catalytic, signal peptide, hinge region, and propeptide region), of which the catalytic domain with active site and zinc-binding region plays a critical role in enzyme activity and the fibronectin site is key for substrate binding and degradation (Huang 2018). The hemopexin-like domain is critical for specificity during recognition and interacts with gelatin and collagen (Roeb et al. 2002). Further, this domain is key in forming a complex with tissue inhibitor of metalloproteinases (TIMPs) and preventing the activation of MMP-9 (Nagase et al. 2006; Ethell, Ethell 2007; Roderfeld et al. 2007; Yabluchanskiy et al. 2013). Due to its proteolytic cleavage activity, MMP-9 modifies cell-cell and cell-ECM interactions, cleaves cell surface proteins and proteins in the extracellular environment, and functions in the proteolytic degradation of ECM (Vandooren et al. 2013; Reinhard et al. 2015; Backstrom et al. 1996; Stamenkovic 2003; Farina, Mackay 2014; Fiore et al. 2002; Vaisar et al. 2009; Hou et al. 2014; Ozdemir et al. 1999; Misko et al. 2002; Hsu et al. 2016; Kim et al. 2012; Dwivedi et al. 2009; Ortega et al. 2005). MMP-9 degrades Type IV collagen and consequently effects basement membrane degradation, the crucial step in tumor invasion and metastasis (Hou et al. 2014; Misko et al. 2002; Ozdemir et al. 1999).

About two decades ago, production of MMP9 by NB cells; its role in induced angiogenesis, tumor progression, and metastasis; and association of MMP9 with advanced disease stage and poor clinical outcomes were documented (Sugiura et al. 1998; Ribatti et al. 1998; Ara et al. 1998). Since then, a growing number of studies have reiterated the role of MMP9 in NB progression and poor clinical outcomes with the recognition of mechanisms and cellular functions involved (Li et al. 2020; Sans-Fons et al. 2010; Cheng et al. 2005). Consistently, global efforts were focused on identifying lead therapeutic deliverables that could target activated MMP9 signaling in NB (Li et al. 2020; Xu et al. 2019; Farabegoli et al. 2018). Conversely, studies from our lab and others have showed therapeutic pressure-associated acquired molecular rearrangements, clonal selection, and cellular function, leading to drug resistance, NB evolution, and poor outcomes (Somasundaram et al. 2019; Aravindan et al. 2013b). For instance, therapeutic pressure has been shown to enhance tumor dissemination by facilitating MMP9 expression and metastatic niche (Zenitani et al. 2018). Furthermore, therapy-exposed bone marrow-derived cells prompt MMP9 induction in tumor cells and clonal modification/selection (EMT), and alter their metastatic state (Gingis-Velitski et al. 2011). More importantly, our studies indicated that residual tumor cells after RT present with high levels of MMP9 and a heightened metastatic state in NB and other tumor systems (Aravindan et al. 2013b; Aravindan et al. 2017). However, a greater understanding of the mechanism(s) involved in acquired maintenance and/or activated MMP9 in therapy-surviving cells is warranted for development of an improved and targeted therapeutic strategy for progressive NB that defies the current intensive multi-modal clinical therapy.

The human MMP-9 gene contains 13 exons and 12 introns, and is located in chromosome 20q13.12. Transcriptionally, the MMP-9 gene is regulated by multiple cis acting factors binding to their matched promoter elements. Transcription factors (TFs) for MMP9 include AP-1 (two recognition sites that bind fos/jun family members), ETS (multiple PEA3 elements), SP1, and NFκB (Benbow, Brinckerhoff 1997; Sato, Seiki 1993). However the stand-alone AP1 recognition is not sufficient and requires substantial NFκB and SP-1 recognition for activation (Benbow, Brinckerhoff 1997; Sato, Seiki 1993). For instance, TNFα-induced MMP9 promoter activation mandates AP-1, PEA3, NFκB, and Sp-1 recognition (Lauricella-Lefebvre et al. 1993). However, the role of specific (e.g., NFκB) TFs in MMP9 regulation remains uncharted. As early as the recognition of MMP9's role in NB progression and clinical outcomes (Sugiura et al. 1998; Ribatti et al. 1998; Ara et al. 1998), it has been shown that NFκB-dependent transcriptional activation of MMP9 is key in enhancing basement membrane invasivity in NB (Farina et al. 1999). Consistently, studies have focused on identifying drug deliverables targeting NFκB-dependent transactivation of MMP9 for NB treatment (Yousefi et al. 2012; Yang et al. 2018). We showed that RT profoundly activates NFκB in NB cells, and RT-triggered NFκB is required for induced radioresistance (Veeraraghavan et al. 2011; Aravindan et al. 2011; Madhusoodhanan et al. 2009; Aravindan et al. 2014). Further, we reported that NB cells that survive RT have high MMP9 activation, and selectively targeting RT-induced nuclear translocation of NFκB regulates RT-induced MMP9 in these cells (Aravindan et al. 2013b). However, it is not clear how MMP9 activation is maintained in the therapy-resistant NB cells.

In the present study, we investigated the mechanism(s) of MMP9 activation with therapeutic (RT) pressure in NB cells and how the activated MMP9 is persistently maintained in surviving cells. The

outcomes of this study showed that, at least in post-treatment surviving NB cells, RT-triggered NFκB mediated MMP-9 reinforced ERK- and/or IKK-dependent MMP9-NFκB feedback, thereby maintaining sustained activation of MMP9.

Materials And Methods

Cell culture

The human NB cells SH-SY5Y, MC-IXC, SK-PN-DW and IMR-32 were obtained from ATCC (Manassas, VA). Culture and maintenance of the NB SH-SY5Y, IMR-32, and SK-PN-DW cells were performed as described in our earlier studies (Veeraraghavan et al. 2011; Aravindan et al. 2013a). For passaging and for all experiments, the cells were detached by using 0.25% trypsin/1% EDTA, resuspended in complete medium, counted (Countess, Invitrogen), and incubated in a 95% air/5% CO_2 humidified incubator. For all experiments, the cells were serum-starved by incubating in medium containing 2% serum for at least 12 h, unless otherwise specified.

Radiation and inhibition studies

For RT experiments, cells were exposed to 2Gy using a Gammacell 40 Exactor (Nordion International, Inc., Ontario, Canada) at a dose rate of 0.81Gy/min and were then incubated at 37°C. Mock-irradiated cells were treated identically except that cells were not subjected to RT. Irradiated cells were incubated for an additional 24 h through 72 h. All experiments were repeated at least three times in each group. The influence of RT-induced NFκB-dependent activation of MMP9 in orchestrating the positive feedback cycle (PFC) was investigated by selectively inhibiting RT-induced MMP9 with 10 μM of GM6001 (Galardin/ilomastat; Cayman Chemicals, Ann Arbor, MI), a potent cell-permeable MMP9 inhibitor. Further, MMP9 specificity was cross validated with a broad spectrum (MMP9 non-selective) serine protease inhibitor (Kuyvenhoven et al. 2004) aprotinin (6.64 nM, ~ 0.35 TIU), which competitively and reversibly inhibits the activity of different esterases and proteases (Soleyman-Jahi et al. 2019). Cells were treated with GM6001 or aprotinin for 3 h prior to RT exposure. In addition, as a reference standard for NFκB dependent activation of MMP9, we used Phorbol 12-myristate 13-acetate (PMA, 10 nM, Cayman Chemical), a polyfunctional diterpene phorbol ester. PMA is an activator of protein kinase C and upregulates MMP-9 in a PKCα-NF-κB dependent manner (Shin et al. 2007).

Plasmid preparation, DNA transfection, and luciferase reporter assay

NFκB p65 and p50 subunits were transiently transfected into the NB cells following the lipofection method utilizing EffecteneTM reagent (Qiagen) as in our earlier studies (Mohan N et al. 2002). NFκB inhibition was achieved using transient transfection of s32A/s36A double mutant IκBα (ΔIκBα) as discussed earlier (Aravindan et al. 2013b). The mutated form of IκBα with a serine-to-alanine mutation at residues 32 and 36 does not undergo signal-induced phosphorylation, and thus remains bound to NFκB, subsequently preventing nuclear translocation and DNA binding. MMP9 overexpression with full-length human untagged MMP9 expression vector and MMP9 inhibition with human MMP9 shRNA plasmid kit (4

unique 29mer constructs) in retroviral RFP vector (Origene, Rockville, MD) were achieved by transient transfection utilizing TurboFectin transfection reagent. In addition, the plasmid construct pNFκB-Luc was amplified, purified, and transfected as in our earlier studies (Aravindan et al. 2013b). Cell lysates were assayed for luciferase activity as per the manufacturer's protocol (Biovision Research Products, Mountain View, CA).

Gelatin zymography

SH-SY5Y, MC-IXC, and IMR-32 cells seeded in 100-mm plates were irradiated and the conditioned medium (CM) was collected after 24, 48, and 72 h. CM collected from mock-IR plates at 72 h was used as controls. CM was concentrated using nanosep 30K concentrators (Pall Biotech, Westborough, MA), and an equivalent volume was subjected to 10% SDS-PAGE containing gelatin (2 mg/ml). The gels were washed in 2.5% Triton X-100 (3X) and incubated in the buffer (50 mM Tris–HCl, pH 7.6; 10 mM $CaCl_2$; 50 mM NaCl and 0.05% Brij35) for 16 h at 37 °C. Gels were then stained with Coomassie brilliant blue R-250 (0.25% in 40% methanol and 10% acetic acid). The MMP activities were visualized as digested bands in a Canon RE350 video visualizer.

Kinetics of MMP9 activity using a fluorogenic substrate

The kinetics of MMP9 activity were measured using a specific fluorogenic substrate (DNP-Pro-Leu-Gly-Leu-Trp-Ala-D-Arg-NH2, Calbiochem), a peptide with the fluorescence on one end and a quencher on the other. After the cleavage into two separate fragments by MMP, the fluorescence is reclaimed and can be quantified in real-time. Equal volumes of CM from the SH-SY5Y, IMR-32, and MC-IXC cells exposed to mock-IR or RT (2Gy) were collected after 2 h (selected for MMP9 activity) and concentrated using nanosep 30K concentrators (Pall Biotech). Concentrated CM (20 µL) in duplicate were mixed with fluorogenic substrate (20 µM, dissolved in DMSO) in 96-well plates for a total volume of 50 µL using assay buffer (0.5 M Tris-HCl, pH 7.7; 5 mM $CaCl_2$; 0.2 M NaCl). Kinetics of the MMP9 activity were immediately and continuously (every 20 minutes for 20 h) quantified by measuring the fluorescence intensity (excitation 280 nm; emission 360 nM) using a Synergy II micro plate reader (Biotek). Group-wise comparisons of MMP9 activity were performed using GraphPad Prism.

Immunoblotting

Total protein extraction and immunoblotting were performed as described in our earlier study (Veeraraghavan et al. 2011). The protein-transferred membranes were incubated with mouse monoclonal anti- MMP-9, IKKβ, p65 (Santa Cruz Biotechnology, Inc., Santa Cruz, CA), rabbit polyclonal anti- ERK and phosphor ERK antibodies, and developed with the appropriate anti-mouse/anti-rabbit antibodies (BioRad Laboratories, Hercules, CA). Blots were stripped and reblotted with mouse monoclonal anti-α-tubulin antibody (Santa Cruz) to determine equal loading of the samples. Band intensity analysis was quantified using Quantity One 1D image analysis software (BioRad). Group-wise comparisons were performed using GraphPad Prism.

Cell-microarray construction and immunohistochemistry

The cell microarray (CMA) approach allows us to measure changes in protein translation across the treated samples, without inter-sample assay discrepancies. For this, human IMR-32 cells (i) exposed to mock-IR, (ii) RT (2Gy), (iii) PMA, (iv) after ectopic expression of p50/p65, (v) treated with GM6001 and exposed to RT, (vi) treated with aprotinin and exposed to RT, and (vii) transfected with ΔIkB and exposed to RT were collected 24 h post-RT. CMA construction, sectioning, and IHC were performed in our Tissue Pathology Core of the Stephenson Cancer Center following standard protocols, as described in our earlier work (Somasundaram et al. 2019). Appropriate histology controls (H&E) and negative controls with no primary antibody were examined in parallel. Expression and localization of MMP9, NFκB- p105, RelB, pP65, p65, IκBα, pIκBα, ERK, and pERK are investigated. The slides were digitally scanned into virtual slides using a Zeiss Axio Scan Z1 slide scanner at 40× magnification. The whole slide images were then group-analyzed for protein-specific positivity using Aperio image analysis and quantification software (Aperio Technologies, Inc., Buffalo Grove, IL, USA) with the appropriate algorithms for protein specific cellular localization. Group-wise comparisons were performed using GraphPad Prism.

MAP kinase/ERK kinase assay

MMP9-dependent modulation of RT-altered ERK activity was assessed using a MAP kinase/ERK immunoprecipitation kinase assay kit (Millipore Sigma, Burlington, MA) following the manufacturer's protocol. First, anti-MAPK/Erk1/2 agarose conjugate was washed (2X) and re-suspended in assay buffer (50 mM Tris, pH 7.5; 1 mM EDTA; 1 mM EGTA; 0.5 mM Na_3VO_4; 0.1% 2-mercaptoethanol; 1% Triton X-100; 50 mM sodium fluoride; 5 mM sodium pyrophosphate; 10 mM sodium beta-glycerol phosphate; 0.1 mM PMSF; 1 ug/mL aprotinin; 1 ug/mL pepstatin; 1 ug/mL leupeptin; 1 uM microcystin). Fresh lysates (500 µg) from cells exposed to mock-IR; RT with/without aprotinin, GM6001, ΔIκBα; NFκB overexpressed; or treated with PMA were added to the anti-MAPK/Erk1/2 agarose conjugate and were allowed to form an immunocomplex for 2 h at 4 °C. The immunocomplex was washed in assay buffer (3X) and in assay dilution buffer (2X, 20mM MOPS, pH 7.2; 25 mM β-glycerol phosphate; 5mM EGTA; 1mM sodium orthovanadate; 1mM dithiothreitol). An aliquot (10 µL) of the agarose/enzyme immunocomplex was mixed with inhibitor cocktail, MAP Kinase/Erk Substrate Cocktail II, and Mg2+/ATP Cocktail in assay dilution buffer and incubated for 20 minutes at 30 °C. The samples were then resolved in SDS-page gel, transferred to PVDF, and labelled with anti-phospho MBP. Band intensity analysis was quantified using Quantity One 1D image analysis software (BioRad). Group-wise comparisons were performed using GraphPad Prism.

Cell death (TUNEL) analysis

RT-triggered NFκB-dependent MMP9 activation and maintenance-associated induced NB cell death, if any, was quantified at the single-cell level based on labeling DNA strand breaks with terminal deoxynucleotidyl transferase (TUNEL Assay). All TUNEL assay procedures were performed on the customized CMA (constructed as discussed above) in the SCC-Tissue Pathology Core using a

commercially available *In Situ cell death detection kit* (MilliporeSigma, St. Louis, MO, USA). Appropriate positive (recombinant DNAse I treatment before TUNEL labeling) and negative (without Tdt enzyme mix) controls were included. The slides were micro-digitally scanned using an Aperio Scanscope (Aperio Technologies, Inc., Buffalo Grove, IL, USA) slide scanner. TUNEL positivity was observed using NIH ImageJ, plotted with GraphPad Prism, and compared between groups using ANOVA with Tukey's post-hoc correction.

QPCR profiling of tumor invasion/metastasis signaling and bioinformatics analysis

Total RNA extraction and real-time QPCR profiling were performed as described in our earlier studies (Aravindan et al. 2013b). We used our custom archived human tumor invasion and metastasis signaling pathway profiler (Realtimeprimers.com, Elkins Park, PA) containing 93 genes to assess the direct effect of RT-induced MMP9 in orchestrated tumor progression. Twenty-seven of the included genes (CD44, CCR7, CTSB, CTSL1, EREG, HGF, ID1, IL1B, KISS1, MCAM, MMP1, MMP13, MMP3, MMP9, MYC, NF2, NME4, PTEN, PTGS2, SERPINE1, SPARC, SPP1, SYK, TIMP2, TNC, TP53, and VEGFA) are known to contain NFκB response elements, allowing us to define how MMP9 alteration modifies the NFκB-dependent response. The ΔΔct values were calculated by normalizing the gene expression levels to positive controls (β-actin, GAPDH, Hprt1), compared between groups, and the relative expression level of each gene was expressed as a fold change. Differential gene expression analysis with stringent criteria (log2 fold change) coupled with false discovery rate calculation were used identify the genes altered with RT, with and without inhibition of RT-activated MMP9. To investigate the functional relevance of modulated genes in tumor progression, we utilized ingenuity pathway analysis (IPA). Core analysis on the genes that showed significant differential changes with/without MMP9 after RT were selectively annotated (defined or predicted data availability) and subjected to downstream analysis by the IPA. Core analysis was performed with criteria including a direct relationship with causal path scoring for networks and upstream regulator analysis and experimentally observed confidence level. Significant associations of the genes with diseases, molecular and cellular functions, and canonical pathways and networks were examined.

Results

RT triggered and maintained MMP9 activity in surviving NB cells

To define whether a clinically relevant dose of RT triggers and maintains MMP9 activity, NB cells (SH-SY5Y, IMR-32, and MC-IXC) exposed to RT (2Gy) were assessed for changes in MMP9 activity at 24 through 72 h post-RT (Fig. 1A). Zymography analysis revealed a robust increase in MMP9 activity in all NB cells investigated. The induced MMP9 activity was maintained consistently at 48 and 72 h. Interestingly, a similar increase in and maintenance of MMP2 activity was observed in those cells that survived RT. Further, (i) to shed light on the triggering time line of MMP9 activity after RT; (ii) whether activation is transient or persistent; and (iii) temporal fluctuations (phases) of activity, if any, we assessed the kinetics of MMP9. Mock-irradiated controls showed a stable cell line-independent and time-independent base-line MMP activity. Compared with mock-IR, RT profoundly increased MMP9 activity in

these cells (Fig. 1B). Interestingly, the heightened MMP9 activity peaked around 4–6 hours. This increased activity was persistently maintained for at least for 20 h without any time-dependent fluctuations/phases (Fig. 1B). These results corroborate well with the zymography results, where we observed a significant maintenance of MMP9 activity even after 72 h. PMA was used as control to assess the magnification of RT-induced/maintained MMP9 activity. While RT-induced activity is near-50% of PMA- induced activity in SH-SY5Y and identical in IMR-32, the activity is robust in MC-IXC in relation to PMA treatment (Fig. 1B). To define the MMP9 specificity, we examined the activity kinetics in cells pretreated with GM6001 (synthetic MMP inhibitor) prior to RT. Treatment with GM6001 completely reverted the observed RT-triggered and maintained MMP9 activity (Fig. 2A). GM6001-affected MMP9 activity is consistent and near-baseline (mock-IR) levels in all three cell lines investigated (Fig. 2A). On the other hand, aprotinin treatment did not revert RT-induced/maintained MMP9 activity to near-baseline levels (data not shown).

To examine whether RT affects the translation of MMP9 (beyond the altered activity) in surviving NB cells, we assessed MMP9 expression through immunoblotting in MC-IXC and SK-PNDW cells, and by CMA-IHC in IMR-32 cells. Compared with the mock-IR controls, RT significantly increased MMP9 translation in all three cell lines investigated (Figs. 2B-D; 3A-B). Similarly, we observed a significant increase in MMP9 translation in all three NB cells treated with PMA. Furthermore, GM6001 treatment completely inhibited RT-induced translation of MMP9, at least in IMR-32 and SK-PNDW cells (Figs. 2B-D; 3A-B). Treatment with aprotinin did not inflict any reduction in RT-induced MMP9 expression in MC-IXC, SK-PN-DW, and IMR-32 cells, and served as the specificity control for GM6001-inhibited MMP9. Together, these results show that clinical doses of RT increased and maintained the MMP9 enzyme activity, as well as the protein translation, in surviving NB cells.

RT-induced MMP-9 actuated NFκB signaling and NFκB transcriptional activity

In our previous studies, we reported that clinical doses/regimen of RT profoundly activate NFκB (Aravindan et al. 2013b; Veeraraghavan et al. 2011; Aravindan et al. 2011; Madhusoodhanan et al. 2009; Aravindan et al. 2014) and further unveiled the NFκB-dependent signaling mechanisms of survival advantage in NB. Herein, we investigated whether RT-triggered NFκB orchestrates MMP9-dependent feedback for the maintenance of MMP9 activity. Immunoblotting in MC-IXC and SK-PN-DW (Fig. 2B-D) and CMA-IHC in IMR-32 (Fig. 4A-B) showed a significant increase in the expression of NFκB p50 and p65 and phosphorylation of p65. In addition, we observed a significant increase in the expression of other NFκB family (RelB and p105) proteins (Fig. 4A-B). Conversely, treating cells with GM6001 significantly inhibited RT-induced p50, p65, RelB, and p105 in all three NB cell lines investigated (Fig. 2B-D; Fig. 4A-B). Interestingly, we observed a significant inhibition in IMR-32 and SK-PN-DW cells, but not in MC-IXC cells. On the other hand, PMA (which activates MMP9) resulted in a significant increase in p50 and p65 expression and p65 phosphorylation in NB cells, indicating that MMP9 activation could lead to increased expression and phosphorylation of p65. Further, to validate whether MMP9-induced expression and phosphorylation of p65 translates the transcriptional activity of NFκB, we performed an NFκB luciferase assay (Fig. 4C). Compared with mock-IR controls, RT significantly ($P < 0.005$) increased NFκB

transcriptional activity in NB cells. shRNA-mediated silencing of MMP9 resulted in complete (near-baseline) inhibition of RT-induced NFκB transcriptional activity (Fig. 4C). Conversely, forced expression of MMP9 in NB cells showed a robust ($P < 0.002$) increase in NFκB activity when compared with the mock-IR. This MMP9-dependent increase in transcriptional activity is significantly ($P < 0.008$) repressed in the presence of GM6001 (Fig. 4C). Together, these results clearly indicate that RT activated MMP9 prompts NFκB expression and/or phosphorylation, which lead to increased NFκB transcriptional activity.

RT-triggered NFκB orchestrated the NFκB-MMP9 feedback cycle

Recognizing that (i) RT-induces NFκB transcriptional activity, (ii) MMP9 have NFκB binding sites, and (iii) RT-induced MMP9 causally orchestrates a feedback loop to NFκB (Figs. 2 and 4), it is pertinent to understand the causal therapeutic pressure trigger. The hypothesis is that therapy (RT)-triggered NFκB orchestrates the MMP9-NFkB positive feedback cycle, which leads to the maintenance of high enzyme activity and tumor evolution. Changes in RT-induced MMP9 expression and activity were examined after selectively inhibiting the nuclear translocation of p65. Cells transfected with ΔIκBα (s32A/s36A double mutant IκBα) and exposed to RT showed a significant decline in the levels of RT-phosphorylated p65 (Fig. 2B-D). Consistently, we observed a significant decrease in RT-induced MMP9 expression in NB cells. Likewise, MMP9 activity analysis showed complete inhibition (near-identical to mock-IR) of MMP9 activity in all NB cells transfected with ΔIκBα (Fig. 5). Conversely, forced expression of p50/p65 in neuroblastoma cells significantly increased MMP9 expression (Fig. 2B-D) and MMP9 enzymatic activity (Fig. 5) when compared with the mock-IR exposed cells. The expression and activity was near-identical to the levels induced by RT. Together, these results indicate that RT-induced NFκB is required for the RT-induced NFkB-MMP9-NFkB feedback cycle.

MMP9 regulated NFκB through IKK and ERK signaling

To understand the mechanism by which RT triggered NFκB-dependent MMP9 feedback NFκB activation, we explored its role in altering NFκB canonical signaling. Since IKKβ is specific for NFκB canonical signaling (IKKα is for non-canonical signaling), we investigated its modification, if any, in NB cells, with and without blocking RT-induced MMP9. Compared with the mock-IR controls, we observed a significant increase in IKKβ localization in cells exposed to RT and in cells with forced expression of p50/p65. Muting RT-induced MMP9 with GM6001 resulted in completely reduced levels of IKKβ in both NB cell lines investigated (Fig. 2B-D). Consistent with the MMP9-dependent regulation of IKKβ, we found a substantial decrease in the IκBα phosphorylation when compared with RT (Fig. 6). Total IκBα levels were high in GM6001-treated RT-exposed cells as opposed to the cells with only RT exposure, indicating the loss of IKKβ-dependent phosphorylation. Next, assessing the effect of MMP9 on ERK activity and ERK-dependent NFκB activation, we examined the levels of ERK phosphorylation in NB cells. Compared with the mock-IR control, RT significantly increased the phosphorylation of ERK in MC-IXC, SK-PN-DW (Fig. 2B-D), and IMR-32 cells (Fig. 7). Forced expression of p50/p65 in these cells showed a significant increase in ERK phosphorylation and served as the positive control. However, muting RT-induced MMP9 with GM-6001 partly inhibited RT-induced ERK phosphorylation (Figs. 2B-D; 7A-B). Directly assessing the active

ERK/phosphotransferase immune complex, we found significant ERK activity in cells that survived RT (Fig. 7C). More importantly, when we silenced the RT-induced MMP9, the RT-induced ERK phosphotransferase activity was completely reduced ($P < 0.001$). Conversely, cells treated with PMA showed a significant increase in ERK activity when compared with mock-IR control (Fig. 7C). Together, these results indicate that RT-induced MMP9 regulates NFκB through IKKβ in one part and through ERK on the other, at least in the NB setting.

Role of RT-triggered NFκB-dependent MMP9 in NB evolution

It has been reported that targeting MMP9 could prompt NFκB regulation-dependent apoptosis. To determine whether RT-triggered NFκB-MMP9-NFκB PFC-dependent activation of MMP9 contributes to tumor evolution, we examined the apoptotic alterations in NB cells exposed to RT with/without MMP9 blocking. Compared with the mock-IR controls, RT significantly induced apoptosis (Fig. 8A-B). However, when RT-induced MMP9 was inhibited, we observed a robust increase in NB cell death *(vs.* RT), indicating that MMP9-dependent NFκB activation regulates RT-induced cell survival.

Activated MMP9 heavily contributes to tumor invasion and metastasis through matrix degradation. However, its role in tumor progression beyond its enzymatic reaction is thus far unrealized. We examined the effect of RT-induced NFκB-MMP9-NFκB PFC-dependent MMP9 in facilitating tumor invasion and dissemination beyond ECM degradation. Examining 93 tumor invasion and metastasis signaling genes, we observed a heightened metastatic state of NB cells that survive RT, with 31 genes showing significant upregulation (Fig. 9A). Nineteen of 31 RT-upregulated genes were downregulated when cells were treated with GM6001 and exposed to RT (Fig. 9B and C). RT induced MMP9 in NB cells and this RT-induced MMP9 was downregulated in the presence of GM6001 (Fig. 9C). Interestingly, seven (ID1, ILIB, KISS1, MCAM, MMP1, MMP9, VEGFA) of 19 genes regulated in the presence of GM6001 are known to contain NFκB response elements. Ingenuity pathway core analysis revealed that this small subset of tightly inter-regulated molecular targets showed influential participation in many canonical signaling pathways and demonstrated defined roles in tumor invasion and metastasis. IPA-data mining considering only relationships where confidence = experimentally observed; these molecules exhibited their role in at least 245 different canonical pathways exerting nearly 150 biological functions. Interestingly, in light of tumor progression and dissemination, we observed a significant association (-log(p-value)) of these molecules in key pathways including the tumor microenvironment, role of tissue factor in cancer, HIFα signaling, HOTAIR regulatory pathway, regulation of the EMT by growth factors pathway, regulation of EMT pathway, stat3 pathway, epithelial adherens junction signaling, molecular mechanisms of cancer, NFκB signaling, IGF signaling PPAR signaling, RAR activation, mTOR signaling, and cancer drug resistance (Additional file 1: Figure S1; Table S1). An all-encompassing overview of these molecules, including information on their symbol, name, subcellular location, protein functions, binding, regulating, regulated by, targeted by miRNA, role in cell, molecular function, biological process, cellular component, disease, and role in tumor progression and metastasis, are provided in Additional file 2: Table S2.

Discussion

Understanding the acquired molecular rearrangements in therapy-surviving cells is critical in developing improved therapeutic measurements for the progressive NB that defies current clinical therapy. We provided first evidence that clinically relevant fractionated RT activates NFκB in surviving NB cells (Aravindan et al. 2008; Madhusoodhanan et al. 2009). Further, our studies unveiled NFκB-dependent intra- and inter- cellular mechanisms that coordinate survival advantage, clonal expansion, and tumor progression (Aravindan et al. 2011; Veeraraghavan et al. 2011; Aravindan et al. 2013a; Aravindan et al. 2013b; Aravindan et al. 2014). In the present study, we investigated how RT-activated NFκB contributes to tumor dissemination and the signaling mechanisms involved in the cause-effect. Our results indicate that RT increases MMP9 expression and enzyme activity. Therapeutic pressure-associated activation of MMP9 has been realized in many cancers (Zhang et al. 2015; Yang et al. 2003). An RT-associated increase in MMP9 activity and its functional role in tumor invasion and metastasis has been documented in numerous cancers, including lung cancer, breast cancer, medulloblastoma, and meningioma (Gogineni et al. 2009; Asuthkar et al. 2014; Chou et al. 2012). In NB, we have shown that RT-induced NFκB facilitates MMP9 activation (Aravindan et al. 2013b). Consistently, a study from Jadhav and Mohanam indicated that RT-induced MMP9 could contribute to NB cells' invasiveness and angiogenesis of human microvascular endothelial cells (Jadhav, Mohanam 2006). However, the mechanism(s) by which MMP9 is activated after RT and how activated MMP9 translates to invasiveness and tumor progression are thus far unrealized. Our results, for the first time, clearly indicate that the clinical dose of RT not only activates MMP9 in NB cells, but also leads to the persistent maintenance of increased enzyme activity in these cells.

Consistent with our earlier studies (Aravindan et al. 2008; Madhusoodhanan et al. 2009; Veeraraghavan et al. 2011; Aravindan et al. 2013a; Aravindan et al. 2013b; Aravindan et al. 2014), the results presented here show significant activation of NFκB in NB cells after RT exposure. RT-induced NFκB and the signaling involved in tumor cells has been extensively documented over the years, and is beyond the scope of the current study. However, our results demonstrated that RT-induced NFκB is required for the activation and maintenance of MMP9 in this setting. As discussed earlier, MMP-9 is transcriptionally regulated by multiple TFs, including AP-1, ETS, SP1, and NFκB (Benbow, Brinckerhoff 1997; Sato, Seiki 1993). It is also evident that AP1 or other TFs-driven MMP9 transcription require substantiation of NFκB recognition (Benbow, Brinckerhoff 1997; Sato, Seiki 1993) (Lauricella-Lefebvre et al. 1993). Conversely, our present data demonstrate that inhibiting RT-induced NFκB transcriptional activity by blocking IκB phosphorylation completely prevents MMP9 expression and consequent activity. A forced increase of p50/p65 in these cells mimicked the RT-induced effect on MMP9 expression. In parallel, the use of PMA, which is known to upregulate MMP9 through the PKCα-NFκB cascade, serves as the best positive control for the study (Shin et al. 2007). These outcomes indicate that RT-induced NFκB is both required and adequate to activate MMP9 in NB cells.

More importantly, the results presented here revealed that RT-triggered and -maintained MMP9 enzyme activity facilitates the onset of second signaling feedback to NFκB. We showed that blocking RT-triggered NFκB-dependent MMP9 resulted in the regulation of NFκB family proteins and reduced phosphorylation of p65. Rao and colleagues indicated that targeting MMP9 inhibits RT-induced NFκB and consequently

affected apoptosis in a breast cancer setting (Kunigal et al. 2008). For the first time, here we showed that MMP9 activity corroborates with the NFκB transcriptional activity in NB cells and beyond. Our outcomes from the NFκB luciferase assay showed a significant decrease in RT-induced NFκB transcriptional activity in both MMP9-muted cells and in cells treated with GM6001. Substantiating our observations, studies have shown that NFκB activation was prevented by selective MMP9 inhibition (Kunigal et al. 2008; Dwir et al. 2020). More importantly, our results indicated that forced expression of MMP9 in NB cells perpetrates a robust NFκB transcriptional activity. To our knowledge, for the first time, our results portray that activated MMP9 communicates with the NFκB signaling pathway and leads to increased NFκB transcriptional activity. Earlier, we showed that blocking RT-induced second-signaling feedback-associated nuclear translocation of NFκB completely prevented the activation of MMP9 (Aravindan et al. 2013b). These outcomes reveal the existence of NFκB→MMP9→NFκB PFC after a clinical dose of RT in NB cells and the requirement of this RT-triggered second signaling feedback for persistent maintenance of heightened MMP9 activity.

Considering the existence of NFκB→MMP9→NFκB PFC after RT in surviving tumor cells, it is pertinent to understand the signaling mechanism by which activated MMP9 actuates the NFκB signaling. Our results indicated that RT-induced MMP9 communicates with the NFκB signaling cascade through IKK and/or ERK signaling. First, our results recognized the reversal of RT-induced ERK phosphorylation when we selectively blocked the RT-induced MMP9. We and others have shown that RT induces ERK phosphorylation in surviving tumor cells (Aravindan et al. 2013c; Ala et al. 2020; Lu et al. 2020). Likewise, regulation of ERK phosphorylation by MMP9 in the presence and/or absence of RT has been previously documented (Bhoopathi et al. 2008; Kunigal et al. 2008; Gogineni et al. 2009). Interestingly, definitive direction of MMP9-dependent ERK-phosphorylation regulation is more of cell/tumor-type dependent. Rao and colleagues showed that MMP9 activates ERK in breast cancer (Kunigal et al. 2008), whereas MMP9 affects ERK phosphorylation in medulloblastoma (Bhoopathi et al. 2008) and meningioma (Gogineni et al. 2009). Here we provide first evidence that MMP9 activates ERK in NB cells that survive RT. Our results showed high levels of ERK phosphotransferase activity, which is completely lost with selective inhibition of MMP9. Conversely, RT-mimicking levels of ERK phosphotransferase activity with PMA, a NFκB-dependent MMP9 inducer, bolster our claims.

Because ERK activation actuates NFκB signaling by regulating IκK and thereby increasing IκBα phosphorylation (Chen et al. 2016), we next investigated the effect of RT-activated MMP9 on IKK signaling and IκB phosphorylation. The IKK complex is the pivotal regulator of inducible NFκB signaling and includes a regulatory sub-unit NEMO and two kinases, IKKα and IKKβ. While NEMO and IKKβ contribute to the canonical NFκB signaling pathway, IKKα facilitates non-canonical mechanisms (Solt, May 2008). To that end, our results showed a significant induction of IKKβ in irradiated cells, while this induction was completely alleviated when RT-induced MMP9 activity was inhibited. Substantiating the MMP9-dependency of IKKβ alterations, our results confirmed a significant MMP9-IκB phosphorylation association in NB cells. Together, these outcomes clearly portray the unforeseen role of MMP9 in the second signaling feedback to NFκB activation after RT and suggest that MMP9 exploits ERK- and/or IKKβ-dependent IκBα phosphorylation for the cause-effect (Fig. 10).

MMP9 is known to endorse tumor metastasis by facilitating cellular migration and invasion through the degradation of ECM (Vandooren et al. 2013; Reinhard et al. 2015; Backstrom et al. 1996; Stamenkovic 2003; Farina, Mackay 2014; Fiore et al. 2002; Vaisar et al. 2009; Hou et al. 2014; Ozdemir et al. 1999; Misko et al. 2002; Hsu et al. 2016; Kim et al. 2012; Dwivedi et al. 2009; Ortega et al. 2005). Due to its placement as both a downstream effector and upstream regulator of key oncogenic signaling events (release of EGF, FGF-2, VEGF; modulate integrin and RTKs' function), MMP9 has been implicated in tumor growth and progression (Ardi et al. 2009; Bergers et al. 2000; Deryugina, Quigley 2010; Perng et al. 2011; Bauvois 2012; Beliveau et al. 2010; J 2011) On the note of therapeutic pressure-associated tumor evolution, we assessed the role of RT-induced NFκB-MMP9 PFC in preventing cell death and facilitating dissemination. Blocking RT-induced PFC-dependent persistent maintenance of MMP9 expressively increased NB cell death. Consistently, studies have shown that selective targeting of RT-induced MMP9 promotes cancer cell death in diverse tumor settings, including breast cancer, medulloblastoma, and meningioma (Gogineni et al. 2009; Kunigal et al. 2008; Bhoopathi et al. 2008; Nyormoi et al. 2003).

Next, looking into its upstream regulatory capabilities, our custom archived QPCR profiling identified at least 19 (of 32 RT-activated) tumor evolution-related oncotargets that are specifically regulated by MMP9. Since individually discussing the oncogenic role of each of these 19 MMP9-regulated molecules will be elaborate and is beyond the scope of this study, we examined their integrated role in tumor cell signaling and tumor evolution function. Bioinformatic analysis with IPA clearly portrayed the high significance of these molecules in cancer evolution and drug resistance, with direct implications in 245 canonical signaling and 150 biological functions. Critically, these molecules are directly involved in tumor microenvironment, drug resistance, EMT, survival, clonal selection, progression, and metastasis, directly affecting key pathways such as tissue factors, HIFα, HOTAIR, stat3, IGF, RAR, mTOR, and NFκB. To our knowledge, this is the first report identifying a group of tumor progression targets that could be regulated by MMP9 in NB cells under therapeutic pressure, in this case RT. More importantly, seven (*ID1*, *ILIB*, *KISS1*, *MCAM*, *MMP1*, *MMP9*, *VEGFA*) of the regulated genes are known to possess NFκB binding sites. This affirms that MMP9-dependent second-signaling feedback to NFκB is critical for the transcription of these molecules. Together, these diverse aspects of MMP9 function work in concert to effect the signaling dysregulation in NB cells that survive therapy, and contribute to the resistance, survival, growth, and spread of NB.

The authors acknowledge the limitations of this study, including the requirement for a preclinical animal model coupled with the induction (or maintenance) phase combination chemotherapy appropriate in conjunction with RT for any meaningful clinical translation. However, this proof-of-concept *in vitro* study is warranted, and provides the first evidence on existence of the RT-triggered NFκB-MMP9-NFκB feedback cycle; the PFC-maintained MMP9 activity; and the molecular signaling involved. The authors also acknowledge that the use of single-dose RT is a limitation and a clinically relevant fractionated dose regimen is required. As discussed above, unveiling the existence of the signal transduction will now allow us to translate this to preclinical spontaneous NB *in vivo* systems with mimicking clinical therapy regimens and to measure the influence in real time in light of tumor progression and spreading.

In conclusion, in this study, we report that a clinical dose of RT significantly increases MMP9 activity and the induced activity is persistently maintained across human NB cell lines investigated. Further, we showed that RT triggers NFκB phosphorylation, nuclear localization, and transcriptional activity, and this RT-induced NFκB is required and adequate for the maintenance of MMP9. RT-triggered NFκB-dependent MMP9 actuates a second-signaling feedback to NFκB signaling, thereby facilitating a NFκB-MMP9-NFκB PFC. Our results demonstrated that MMP9-NFκB second signaling feedback is mediated by MMP9-dependent activation of IKKβ and ERK activity. Beyond its regular tumor invasion and metastasis function, PFC-dependent MMP9 activation lessens RT-induced apoptosis through the activation of NFκB signaling. More importantly, this study identified that NFκB-MMP9-NFκB-dependent MMP9 regulates 19 critical molecular determinants that play a pivotal role in tumor evolution. Interestingly, seven of these molecules have binding sites for NFκB, indicating that MMP9 regulates these molecules by activating NFκB. Collectively, these data suggest that acquired maintenance of MMP9 after therapeutic pressure could contribute heavily for tumor evolution, and selective inhibition of activated MMP9 maintenance could serve as a promising therapeutic strategy for progressive NB that defies current clinical therapy.

Declarations

Funding: The National Institutes of Health, NIH-P20GM103639, and Oklahoma Center for the Advancement of Science and Technology, OCAST-HR19-04.

Conflicts of interest: All authors have nothing to disclose.

Availability of data and material: No additional data are available.

Code availability: Not applicable

Author Contributions:

NA contributed to the conception and design of the experiments.

DS, SA, RM, MN, and NA performed the experiments and contributed to the acquisition of the data.

NA, SA, and MN contributed to data analysis and interpretation of the data.

NA and DS drafted the manuscript, and MN helped in revising it critically.

All authors read and approved the final manuscript.

Ethics approval: Not applicable

Consent to participate: Not applicable

Consent for publication: Not applicable

Acknowledgements

The authors acknowledge the Stephenson Cancer Center (SCC) Cancer Tissue pathology core for all CMA IHC and TUNEL services and the SCC Cancer Functional Genomics core for help with whole genome gene expression. The authors also acknowledge the OUHSC Staff Editor (Ms. Kathy Kyler) for the help in critically reviewing this manuscript.

References

1. Ala M, Mohammad Jafari R, Ala M, Agbele AT, Hejazi SM, Tavangar SM, et al. Sumatriptan alleviates radiation-induced oral mucositis in rats by inhibition of NF-kB and ERK activation, prevention of TNF-alpha and ROS release. Arch Oral Biol. 2020;119:104919. doi:10.1016/j.archoralbio.2020.104919.
2. Ara T, Fukuzawa M, Kusafuka T, Komoto Y, Oue T, Inoue M, et al. Immunohistochemical expression of MMP-2, MMP-9, and TIMP-2 in neuroblastoma: association with tumor progression and clinical outcome. J Pediatr Surg. 1998;33(8):1272–8. doi:10.1016/s0022-3468(98)90167-1.
3. Aravindan N, Aravindan S, Pandian V, Khan FH, Ramraj SK, Natt P, et al. Acquired tumor cell radiation resistance at the treatment site is mediated through radiation-orchestrated intercellular communication. Int J Radiat Oncol Biol Phys. 2014;88(3):677–85. doi:10.1016/j.ijrobp.2013.11.215.
4. Aravindan N, Madhusoodhanan R, Ahmad S, Johnson D, Herman TS. Curcumin inhibits NFkappaB mediated radioprotection and modulate apoptosis related genes in human neuroblastoma cells. Cancer Biol Ther. 2008;7(4):569–76. doi:10.4161/cbt.7.4.5534.
5. Aravindan N, Veeraraghavan J, Madhusoodhanan R, Herman TS, Natarajan M. Curcumin regulates low-linear energy transfer gamma-radiation-induced NFkappaB-dependent telomerase activity in human neuroblastoma cells. Int J Radiat Oncol Biol Phys. 2011;79(4):1206–15. doi:10.1016/j.ijrobp.2010.10.058.
6. Aravindan S, Natarajan M, Awasthi V, Herman TS, Aravindan N. Novel synthetic monoketone transmute radiation-triggered NFkappaB-dependent TNFalpha cross-signaling feedback maintained NFkappaB and favors neuroblastoma regression. PLoS One. 2013a;8(8):e72464. doi:10.1371/journal.pone.0072464.
7. Aravindan S, Natarajan M, Herman TS, Aravindan N. Radiation-induced TNFalpha cross signaling-dependent nuclear import of NFkappaB favors metastasis in neuroblastoma. Clin Exp Metastasis. 2013b;30(6):807–17. doi:10.1007/s10585-013-9580-y.
8. Aravindan S, Natarajan M, Herman TS, Awasthi V, Aravindan N. Molecular basis of 'hypoxic' breast cancer cell radio-sensitization: phytochemicals converge on radiation induced Rel signaling. Radiat Oncol. 2013c;8:46. doi:10.1186/1748-717X-8-46.
9. Aravindan S, Ramraj S, Kandasamy K, Thirugnanasambandan SS, Somasundaram DB, Herman TS, et al. Hormophysa triquerta polyphenol, an elixir that deters CXCR4- and COX2-dependent dissemination destiny of treatment-resistant pancreatic cancer cells. Oncotarget. 2017;8(4):5717–34. doi:10.18632/oncotarget.13900.
10. Ardi VC, Van den Steen PE, Opdenakker G, Schweighofer B, Deryugina EI, Quigley JP. Neutrophil MMP-9 proenzyme, unencumbered by TIMP-1, undergoes efficient activation in vivo and catalytically

induces angiogenesis via a basic fibroblast growth factor (FGF-2)/FGFR-2 pathway. J Biol Chem. 2009;284(38):25854–66. doi:10.1074/jbc.M109.033472.

11. Asuthkar S, Velpula KK, Nalla AK, Gogineni VR, Gondi CS, Rao JS. Irradiation-induced angiogenesis is associated with an MMP-9-miR-494-syndecan-1 regulatory loop in medulloblastoma cells. Oncogene. 2014;33(15):1922–33. doi:10.1038/onc.2013.151.
12. Backstrom JR, Lim GP, Cullen MJ, Tokes ZA. Matrix metalloproteinase-9 (MMP-9) is synthesized in neurons of the human hippocampus and is capable of degrading the amyloid-beta peptide (1–40). J Neurosci. 1996;16(24):7910–9.
13. Bauvois B. New facets of matrix metalloproteinases MMP-2 and MMP-9 as cell surface transducers: outside-in signaling and relationship to tumor progression. Biochim Biophys Acta. 2012;1825(1):29–36. doi:10.1016/j.bbcan.2011.10.001.
14. Beliveau A, Mott JD, Lo A, Chen EI, Koller AA, Yaswen P, et al. Raf-induced MMP9 disrupts tissue architecture of human breast cells in three-dimensional culture and is necessary for tumor growth in vivo. Genes Dev. 2010;24(24):2800–11. doi:10.1101/gad.1990410.
15. Benbow U, Brinckerhoff CE. The AP-1 site and MMP gene regulation: what is all the fuss about? Matrix Biol. 1997;15(8–9):519–26. doi:10.1016/s0945-053x(97)90026-3.
16. Bergers G, Brekken R, McMahon G, Vu TH, Itoh T, Tamaki K, et al. Matrix metalloproteinase-9 triggers the angiogenic switch during carcinogenesis. Nat Cell Biol. 2000;2(10):737–44. doi:10.1038/35036374.
17. Bhoopathi P, Chetty C, Kunigal S, Vanamala SK, Rao JS, Lakka SS. Blockade of tumor growth due to matrix metalloproteinase-9 inhibition is mediated by sequential activation of beta1-integrin, ERK, and NF-kappaB. J Biol Chem. 2008;283(3):1545–52. doi:10.1074/jbc.M707931200.
18. Chavali PL, Saini RK, Zhai Q, Vizlin-Hodzic D, Venkatabalasubramanian S, Hayashi A, et al. TLX activates MMP-2, promotes self-renewal of tumor spheres in neuroblastoma and correlates with poor patient survival. Cell death disease. 2014;5:e1502. doi:10.1038/cddis.2014.449.
19. Chen B, Liu J, Ho TT, Ding X, Mo YY. ERK-mediated NF-kappaB activation through ASIC1 in response to acidosis. Oncogenesis. 2016;5(12):e279. doi:10.1038/oncsis.2016.81.
20. Cheng Y, Dong Q, Sun LR, Yang CM, Jiang BX. [Correlation between expression of MMP-2, MMP-9, TIMP-2, TIMP-1 and metastasis of neuroblastoma]. Zhonghua Zhong Liu Za Zhi. 2005;27(3):164–6.
21. Chou CH, Teng CM, Tzen KY, Chang YC, Chen JH, Cheng JC. MMP-9 from sublethally irradiated tumor promotes Lewis lung carcinoma cell invasiveness and pulmonary metastasis. Oncogene. 2012;31(4):458–68. doi:10.1038/onc.2011.240.
22. Deryugina EI, Quigley JP. Pleiotropic roles of matrix metalloproteinases in tumor angiogenesis: contrasting, overlapping and compensatory functions. Biochim Biophys Acta. 2010;1803(1):103–20. doi:10.1016/j.bbamcr.2009.09.017.
23. Dwir D, Giangreco B, Xin L, Tenenbaum L, Cabungcal JH, Steullet P, et al. MMP9/RAGE pathway overactivation mediates redox dysregulation and neuroinflammation, leading to inhibitory/excitatory

imbalance: a reverse translation study in schizophrenia patients. Mol Psychiatry. 2020;25(11):2889–904. doi:10.1038/s41380-019-0393-5.

24. Dwivedi A, Slater SC, George SJ. MMP-9 and – 12 cause N-cadherin shedding and thereby beta-catenin signalling and vascular smooth muscle cell proliferation. Cardiovasc Res. 2009;81(1):178–86. doi:10.1093/cvr/cvn278.
25. Ethell IM, Ethell DW. Matrix metalloproteinases in brain development and remodeling: synaptic functions and targets. J Neurosci Res. 2007;85(13):2813–23. doi:10.1002/jnr.21273.
26. Farabegoli F, Govoni M, Spisni E, Papi A. Epigallocatechin-3-gallate and 6-OH-11-O-Hydroxyphenanthrene Limit BE(2)-C Neuroblastoma Cell Growth and Neurosphere Formation In Vitro. Nutrients. 2018;10(9). doi:10.3390/nu10091141.
27. Farina AR, Mackay AR. Gelatinase B/MMP-9 in Tumour Pathogenesis and Progression. Cancers (Basel). 2014;6(1):240–96. doi:10.3390/cancers6010240.
28. Farina AR, Tacconelli A, Vacca A, Maroder M, Gulino A, Mackay AR. Transcriptional up-regulation of matrix metalloproteinase-9 expression during spontaneous epithelial to neuroblast phenotype conversion by SK-N-SH neuroblastoma cells, involved in enhanced invasivity, depends upon GT-box and nuclear factor kappaB elements. Cell Growth Differ. 1999;10(5):353–67.
29. Fiore E, Fusco C, Romero P, Stamenkovic I. Matrix metalloproteinase 9 (MMP-9/gelatinase B) proteolytically cleaves ICAM-1 and participates in tumor cell resistance to natural killer cell-mediated cytotoxicity. Oncogene. 2002;21(34):5213–23. doi:10.1038/sj.onc.1205684.
30. Fowlkes JL, Enghild JJ, Suzuki K, Nagase H. Matrix metalloproteinases degrade insulin-like growth factor-binding protein-3 in dermal fibroblast cultures. J Biol Chem. 1994;269(41):25742–6.
31. Gingis-Velitski S, Loven D, Benayoun L, Munster M, Bril R, Voloshin T, et al. Host response to short-term, single-agent chemotherapy induces matrix metalloproteinase-9 expression and accelerates metastasis in mice. Cancer Res. 2011;71(22):6986–96. doi:10.1158/0008-5472.CAN-11-0629.
32. Gogineni VR, Kargiotis O, Klopfenstein JD, Gujrati M, Dinh DH, Rao JS. RNAi-mediated downregulation of radiation-induced MMP-9 leads to apoptosis via activation of ERK and Akt in IOMM-Lee cells. Int J Oncol. 2009;34(1):209–18.
33. Hou H, Zhang G, Wang H, Gong H, Wang C, Zhang X. High matrix metalloproteinase-9 expression induces angiogenesis and basement membrane degradation in stroke-prone spontaneously hypertensive rats after cerebral infarction. Neural Regen Res. 2014;9(11):1154–62. doi:10.4103/1673-5374.135318.
34. Hsu CC, Huang SF, Wang JS, Chu WK, Nien JE, Chen WS, et al. Interplay of N-Cadherin and matrix metalloproteinase 9 enhances human nasopharyngeal carcinoma cell invasion. BMC Cancer. 2016;16(1):800. doi:10.1186/s12885-016-2846-4.
35. Huang H. Matrix Metalloproteinase-9 (MMP-9) as a Cancer Biomarker and MMP-9 Biosensors: Recent Advances. Sensors (Basel). 2018;18(10). doi:10.3390/s18103249.
36. J W. Mesencyhme-epithelial interactions in gastrointestinal development and tumorigenesis [PhD] 2011.

37. Jadhav U, Mohanam S. Response of neuroblastoma cells to ionizing radiation: modulation of in vitro invasiveness and angiogenesis of human microvascular endothelial cells. Int J Oncol. 2006;29(6):1525–31.
38. Kalavska K, Cierna Z, Karaba M, Minarik G, Benca J, Sedlackova T, et al. Prognostic role of matrix metalloproteinase 9 in early breast cancer. Oncology letters. 2021;21(2):78. doi:10.3892/ol.2020.12339.
39. Kataoka H, Uchino H, Iwamura T, Seiki M, Nabeshima K, Koono M. Enhanced tumor growth and invasiveness in vivo by a carboxyl-terminal fragment of alpha1-proteinase inhibitor generated by matrix metalloproteinases: a possible modulatory role in natural killer cytotoxicity. Am J Pathol. 1999;154(2):457–68. doi:10.1016/s0002-9440(10)65292-3.
40. Kim YH, Kwon HJ, Kim DS. Matrix metalloproteinase 9 (MMP-9)-dependent processing of betaig-h3 protein regulates cell migration, invasion, and adhesion. J Biol Chem. 2012;287(46):38957–69. doi:10.1074/jbc.M112.357863.
41. Klein T, Bischoff R. Physiology and pathophysiology of matrix metalloproteases. Amino Acids. 2011;41(2):271–90. doi:10.1007/s00726-010-0689-x.
42. Kunigal S, Lakka SS, Joseph P, Estes N, Rao JS. Matrix metalloproteinase-9 inhibition down-regulates radiation-induced nuclear factor-kappa B activity leading to apoptosis in breast tumors. Clin Cancer Res. 2008;14(11):3617–26. doi:10.1158/1078-0432.CCR-07-2060.
43. Kuyvenhoven JP, Molenaar IQ, Verspaget HW, Veldman MG, Palareti G, Legnani C, et al. Plasma MMP-2 and MMP-9 and their inhibitors TIMP-1 and TIMP-2 during human orthotopic liver transplantation. The effect of aprotinin and the relation to ischemia/reperfusion injury. Thromb Haemost. 2004;91(3):506–13. doi:10.1160/TH03-05-0272.
44. Lauricella-Lefebvre MA, Castronovo V, Sato H, Seiki M, French DL, Merville MP. Stimulation of the 92-kD type IV collagenase promoter and enzyme expression in human melanoma cells. Invasion Metastasis. 1993;13(6):289–300.
45. Levi E, Fridman R, Miao HQ, Ma YS, Yayon A, Vlodavsky I. Matrix metalloproteinase 2 releases active soluble ectodomain of fibroblast growth factor receptor 1. Proc Natl Acad Sci U S A. 1996;93(14):7069–74. doi:10.1073/pnas.93.14.7069.
46. Li XY, Huang GH, Liu QK, Yang XT, Wang K, Luo WZ, et al. Porf-2 Inhibits Tumor Cell Migration Through the MMP-2/9 Signaling Pathway in Neuroblastoma and Glioma. Frontiers in oncology. 2020;10:975. doi:10.3389/fonc.2020.00975.
47. London WB, Castel V, Monclair T, Ambros PF, Pearson AD, Cohn SL, et al. Clinical and biologic features predictive of survival after relapse of neuroblastoma: a report from the International Neuroblastoma Risk Group project. J Clin Oncol. 2011;29(24):3286–92. doi:10.1200/JCO.2010.34.3392.
48. Lu Y, Liu B, Liu Y, Yu X, Cheng G. Dual effects of active ERK in cancer: A potential target for enhancing radiosensitivity. Oncology letters. 2020;20(2):993–1000. doi:10.3892/ol.2020.11684.

49. Lukashev ME, Werb Z. ECM signalling: orchestrating cell behaviour and misbehaviour. Trends Cell Biol. 1998;8(11):437–41. doi:10.1016/s0962-8924(98)01362-2.
50. Madhusoodhanan R, Natarajan M, Veeraraghavan J, Herman TS, Jamgade A, Singh N, et al. NFkappaB signaling related molecular alterations in human neuroblastoma cells after fractionated irradiation. J Radiat Res. 2009;50(4):311–24. doi:10.1269/jrr.08110.
51. Matthay KK, Maris JM, Schleiermacher G, Nakagawara A, Mackall CL, Diller L, et al. Neuroblastoma Nat Rev Dis Primers. 2016;2:16078. doi:10.1038/nrdp.2016.78.
52. Misko A, Ferguson T, Notterpek L. Matrix metalloproteinase mediated degradation of basement membrane proteins in Trembler J neuropathy nerves. J Neurochem. 2002;83(4):885–94. doi:10.1046/j.1471-4159.2002.01200.x.
53. Mohan N, TS NA H. Nitric oxide-mediated inhibition of NFkB regulates hyperthermia-induced apoptosis.. 49th Annual meeting of the Radiation Research Society and 20th Annual meeting of the North American Hyperthermia Society. 2002:abstract.
54. Nagase H, Visse R, Murphy G. Structure and function of matrix metalloproteinases and TIMPs. Cardiovasc Res. 2006;69(3):562–73. doi:10.1016/j.cardiores.2005.12.002.
55. Nyormoi O, Mills L, Bar-Eli M. An MMP-2/MMP-9 inhibitor, 5a, enhances apoptosis induced by ligands of the TNF receptor superfamily in cancer cells. Cell Death Differ. 2003;10(5):558–69. doi:10.1038/sj.cdd.4401209.
56. Ortega N, Behonick DJ, Colnot C, Cooper DN, Werb Z. Galectin-3 is a downstream regulator of matrix metalloproteinase-9 function during endochondral bone formation. Mol Biol Cell. 2005;16(6):3028–39. doi:10.1091/mbc.e04-12-1119.
57. Ozdemir E, Kakehi Y, Okuno H, Yoshida O. Role of matrix metalloproteinase-9 in the basement membrane destruction of superficial urothelial carcinomas. J Urol. 1999;161(4):1359–63.
58. Perng DW, Chang KT, Su KC, Wu YC, Chen CS, Hsu WH, et al. Matrix metalloprotease-9 induces transforming growth factor-beta(1) production in airway epithelium via activation of epidermal growth factor receptors. Life Sci. 2011;89(5–6):204–12. doi:10.1016/j.lfs.2011.06.008.
59. Ra HJ, Parks WC. Control of matrix metalloproteinase catalytic activity. Matrix biology: journal of the International Society for Matrix Biology. 2007;26(8):587–96. doi:10.1016/j.matbio.2007.07.001.
60. Reinhard SM, Razak K, Ethell IM. A delicate balance: role of MMP-9 in brain development and pathophysiology of neurodevelopmental disorders. Front Cell Neurosci. 2015;9:280. doi:10.3389/fncel.2015.00280.
61. Ribatti D, Alessandri G, Vacca A, Iurlaro M, Ponzoni M. Human neuroblastoma cells produce extracellular matrix-degrading enzymes, induce endothelial cell proliferation and are angiogenic in vivo. Int J Cancer. 1998;77(3):449–54. doi:10.1002/(sici)1097-0215(19980729)77:3<449::aid-ijc22>3.0.co;2-1.
62. Roderfeld M, Graf J, Giese B, Salguero-Palacios R, Tschuschner A, Muller-Newen G, et al. Latent MMP-9 is bound to TIMP-1 before secretion. Biol Chem. 2007;388(11):1227–34. doi:10.1515/BC.2007.123.

63. Roeb E, Schleinkofer K, Kernebeck T, Potsch S, Jansen B, Behrmann I, et al. The matrix metalloproteinase 9 (mmp-9) hemopexin domain is a novel gelatin binding domain and acts as an antagonist. J Biol Chem. 2002;277(52):50326–32. doi:10.1074/jbc.M207446200.
64. Sans-Fons MG, Sole S, Sanfeliu C, Planas AM. Matrix metalloproteinase-9 and cell division in neuroblastoma cells and bone marrow macrophages. Am J Pathol. 2010;177(6):2870–85. doi:10.2353/ajpath.2010.090050.
65. Santana VM, Furman WL, McGregor LM, Billups CA. Disease control intervals in high-risk neuroblastoma. Cancer. 2008;112(12):2796–801. doi:10.1002/cncr.23507.
66. Sato H, Seiki M. Regulatory mechanism of 92 kDa type IV collagenase gene expression which is associated with invasiveness of tumor cells. Oncogene. 1993;8(2):395–405.
67. Shin Y, Yoon SH, Choe EY, Cho SH, Woo CH, Rho JY, et al. PMA-induced up-regulation of MMP-9 is regulated by a PKCalpha-NF-kappaB cascade in human lung epithelial cells. Exp Mol Med. 2007;39(1):97–105. doi:10.1038/emm.2007.11.
68. Soleyman-Jahi S, Sadeghi F, Afshari Z, Barati T, Ghasemi S, Muhammadnejad S, et al. Anti-neoplastic effects of aprotinin on human breast cancer cell lines: In vitro study. Adv Clin Exp Med. 2019;28(2):151–7. doi:10.17219/acem/89770.
69. Solt LA, May MJ. The IkappaB kinase complex: master regulator of NF-kappaB signaling. Immunol Res. 2008;42(1–3):3–18. doi:10.1007/s12026-008-8025-1.
70. Somasundaram DB, Subramanian K, Aravindan S, Yu Z, Natarajan M, Herman T, et al. De novo regulation of RD3 synthesis in residual neuroblastoma cells after intensive multi-modal clinical therapy harmonizes disease evolution. Scientific reports. 2019;9(1):11766. doi:10.1038/s41598-019-48034-2.
71. Stamenkovic I. Extracellular matrix remodelling: the role of matrix metalloproteinases. J Pathol. 2003;200(4):448–64. doi:10.1002/path.1400.
72. Sternlicht MD, Bissell MJ, Werb Z. The matrix metalloproteinase stromelysin-1 acts as a natural mammary tumor promoter. Oncogene. 2000;19(8):1102–13. doi:10.1038/sj.onc.1203347.
73. Sternlicht MD, Werb Z. How matrix metalloproteinases regulate cell behavior. Annu Rev Cell Dev Biol. 2001;17:463–516. doi:10.1146/annurev.cellbio.17.1.463.
74. Stetler-Stevenson WG. Type IV collagenases in tumor invasion and metastasis. Cancer Metastasis Rev. 1990;9(4):289–303.
75. Sugiura Y, Shimada H, Seeger RC, Laug WE, DeClerck YA. Matrix metalloproteinases-2 and – 9 are expressed in human neuroblastoma: contribution of stromal cells to their production and correlation with metastasis. Cancer Res. 1998;58(10):2209–16.
76. Suzuki M, Raab G, Moses MA, Fernandez CA, Klagsbrun M. Matrix metalloproteinase-3 releases active heparin-binding EGF-like growth factor by cleavage at a specific juxtamembrane site. J Biol Chem. 1997;272(50):31730–7. doi:10.1074/jbc.272.50.31730.
77. Thomasset N, Lochter A, Sympson CJ, Lund LR, Williams DR, Behrendtsen O, et al. Expression of autoactivated stromelysin-1 in mammary glands of transgenic mice leads to a reactive stroma

during early development. Am J Pathol. 1998;153(2):457–67. doi:10.1016/S0002-9440(10)65589-7.

78. Tlsty TD. Cell-adhesion-dependent influences on genomic instability and carcinogenesis. Curr Opin Cell Biol. 1998;10(5):647–53. doi:10.1016/s0955-0674(98)80041-0.
79. Vaisar T, Kassim SY, Gomez IG, Green PS, Hargarten S, Gough PJ, et al. MMP-9 sheds the beta2 integrin subunit (CD18) from macrophages. Mol Cell Proteomics. 2009;8(5):1044–60. doi:10.1074/mcp.M800449-MCP200.
80. Vandooren J, Van den Steen PE, Opdenakker G. Biochemistry and molecular biology of gelatinase B or matrix metalloproteinase-9 (MMP-9): the next decade. Crit Rev Biochem Mol Biol. 2013;48(3):222–72. doi:10.3109/10409238.2013.770819.
81. Veeraraghavan J, Natarajan M, Aravindan S, Herman TS, Aravindan N. Radiation-triggered tumor necrosis factor (TNF) alpha-NFkappaB cross-signaling favors survival advantage in human neuroblastoma cells. J Biol Chem. 2011;286(24):21588–600. doi:10.1074/jbc.M110.193755.
82. Xu Y, Wang X, Guo B, Wang D, Kalvakolanu DV, Chen X, et al. Nonviral Delivery of GRIM-19 Gene Inhibits Tumor Growth with Reduced Local and Systemic Complications. Hum Gene Ther. 2019;30(11):1419–30. doi:10.1089/hum.2019.134.
83. Yabluchanskiy A, Ma Y, Iyer RP, Hall ME, Lindsey ML. Matrix metalloproteinase-9: Many shades of function in cardiovascular disease. Physiology (Bethesda). 2013;28(6):391–403. doi:10.1152/physiol.00029.2013.
84. Yang CC, Lin CC, Hsiao LD, Yang CM. Galangin Inhibits Thrombin-Induced MMP-9 Expression in SK-N-SH Cells via Protein Kinase-Dependent NF-kappaB Phosphorylation. Int J Mol Sci. 2018;19(12). doi:10.3390/ijms19124084.
85. Yang JM, Xu Z, Wu H, Zhu H, Wu X, Hait WN. Overexpression of extracellular matrix metalloproteinase inducer in multidrug resistant cancer cells. Mol Cancer Res. 2003;1(6):420–7.
86. Yousefı M, Ghaffari SH, Soltani BM, Nafissi S, Momeny M, Zekri A, et al. Therapeutic efficacy of silibinin on human neuroblastoma cells: Akt and NF-kappaB expressions may play an important role in silibinin-induced response. Neurochem Res. 2012;37(9):2053–63. doi:10.1007/s11064-012-0827-9.
87. Zenitani M, Nojiri T, Hosoda H, Kimura T, Uehara S, Miyazato M, et al. Chemotherapy can promote liver metastasis by enhancing metastatic niche formation in mice. J Surg Res. 2018;224:50–7. doi:10.1016/j.jss.2017.11.050.
88. Zhang F, Wang Z, Fan Y, Xu Q, Ji W, Tian R, et al. Elevated STAT3 Signaling-Mediated Upregulation of MMP-2/9 Confers Enhanced Invasion Ability in Multidrug-Resistant Breast Cancer Cells. Int J Mol Sci. 2015;16(10):24772–90. doi:10.3390/ijms161024772.

Figures

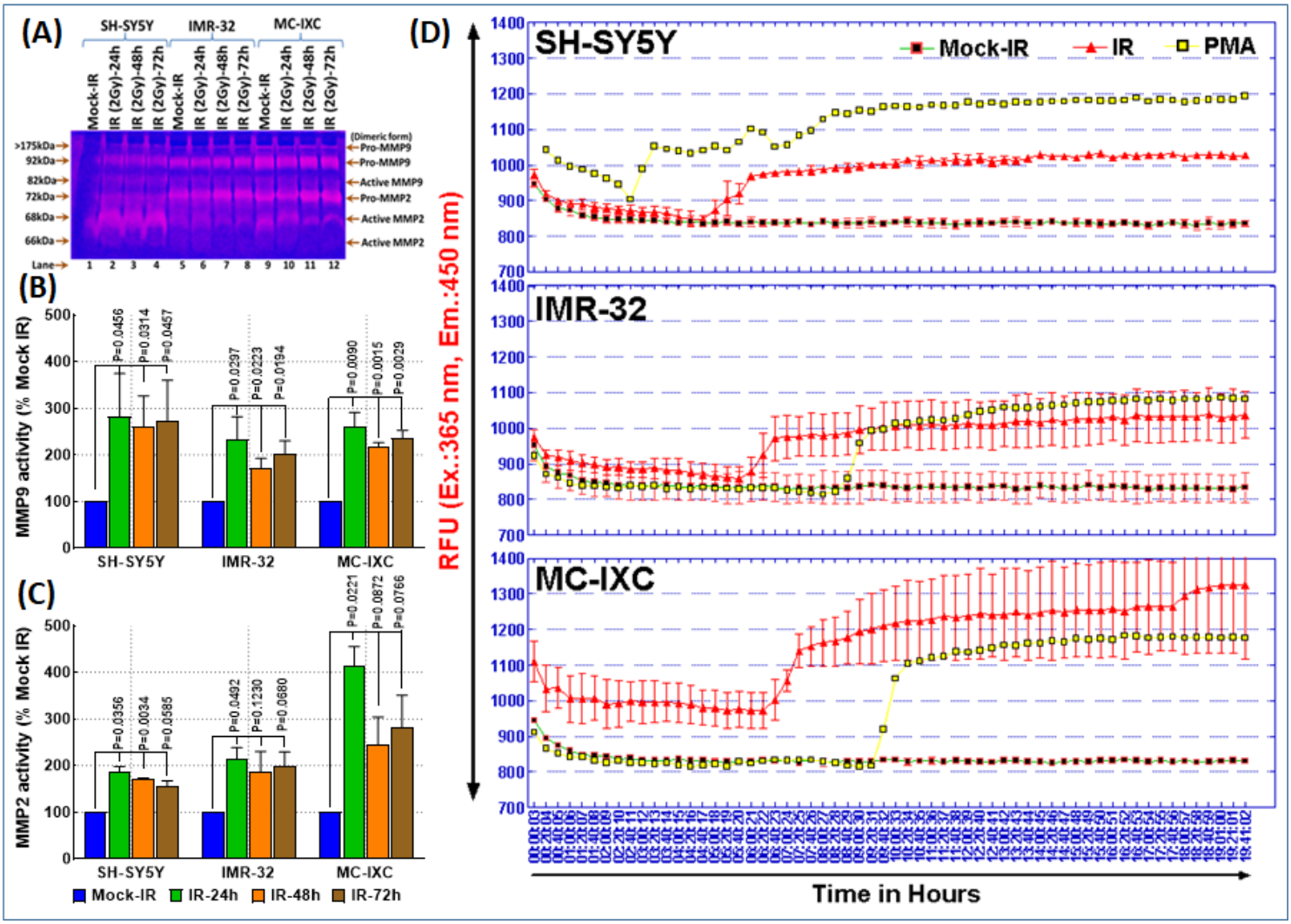

Figure 1

(A) Photograph of gelatin zymography showing MMP9 activity in the conditioned medium of SH-SY5Y, MC-IXC and IMR-32 cells exposed to mock-irradiation or RT (2Gy). MMP9 activity was measured at 24, 48 and 72h post-RT. (B) Line graphs obtained from fluorogenic substrate specific activity assay showing MMP9 activity kinetics in the conditioned medium of NB cells (SH-SY5Y, IMR-32 and MC-IXC) exposed to mock-IR, RT or PMA. Kinetics of the MMP9 activity was continuously (each 20minutes constantly for 20h) quantified by measuring the fluorescence intensity (excitation 280nm; emission 360nM).

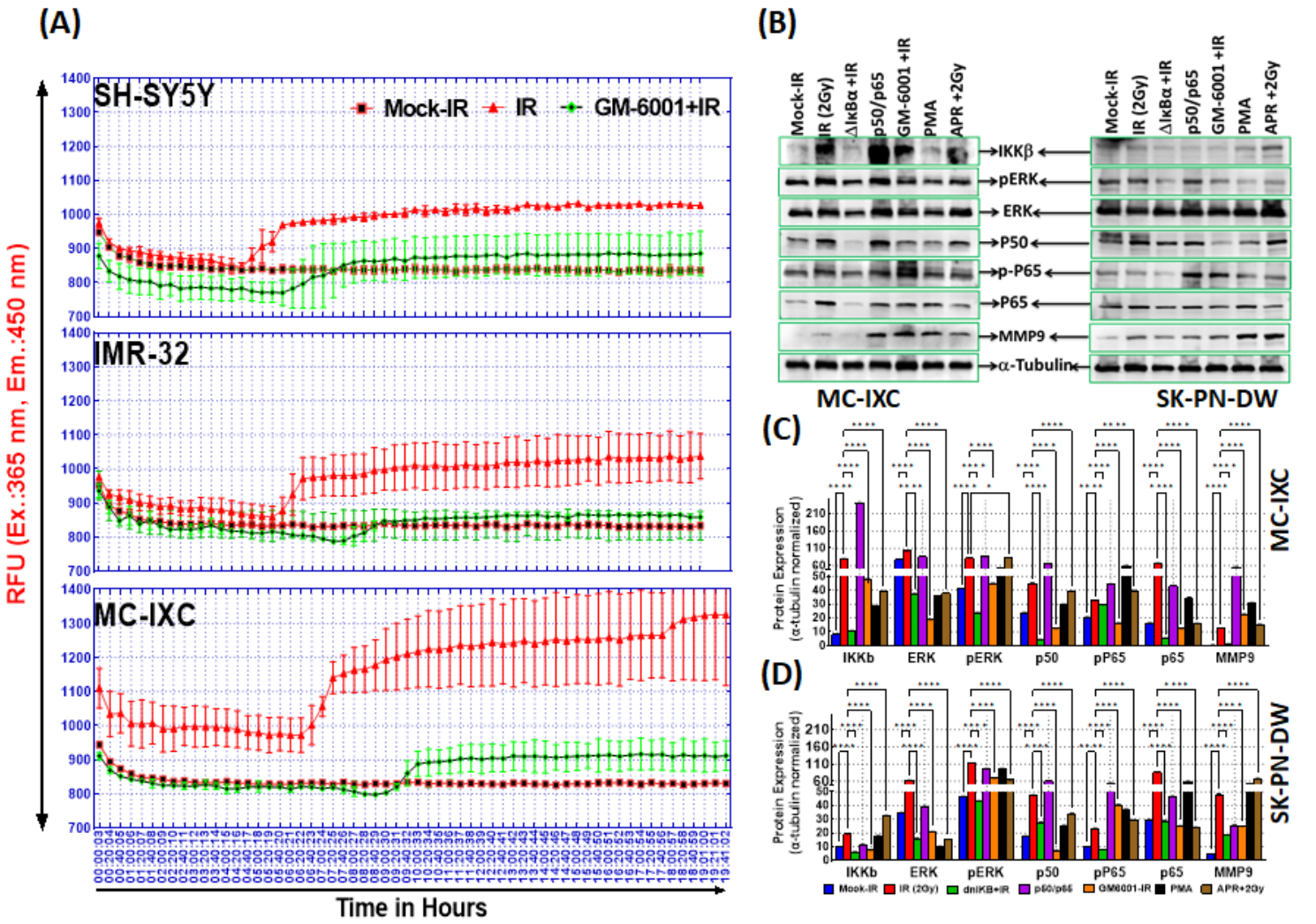

Figure 2

(A) Line graphs obtained from fluorogenic substrate specific activity assay showing MMP9 activity kinetics in the conditioned medium of NB cells (SH-SY5Y, IMR-32 and MC-IXC) exposed to mock-IR, RT or, treated with GM-6001 (a potent cell permeable MMP9 inhibitor) and exposed to RT. Kinetics of the MMP9 activity was quantified continuously for every each 20minutes constantly for 20h. (B) Representative immunoblots showing the expression of IKKβ□□ERK1/2, pERK1/2, NFkB-p50, NFkB-p65, NFkB-p65 phosphorylated, and MMP9 in MC-IXC and SK-PN-DW NB cells exposed to mock-RT, RT (2Gy), PMA, after ectopic expression of p50/p65, treated with GM6001 and exposed to RT, treated with aprotinin and exposed to RT or, transfected with □IkB and exposed to RT. Blots were stripped and reblotted with mouse monoclonal anti-α-tubulin antibody to determine equal loading of the samples. Histograms obtained from 1D gel analysis of immunoblots showing altered levels of IKKβkERK1/2, pERK1/2, NFkB-p50, NFkB-p65, NFkB-p65 phosphorylated, and MMP9 in (C) MC-IXC and (D) SK-PN-DW cells. Levels are expressed as α-tubulin normalized percent change. Graph construction and the group-wise comparison was made in Graphpad Prism. A P value of less than 0.05 is considered significant.

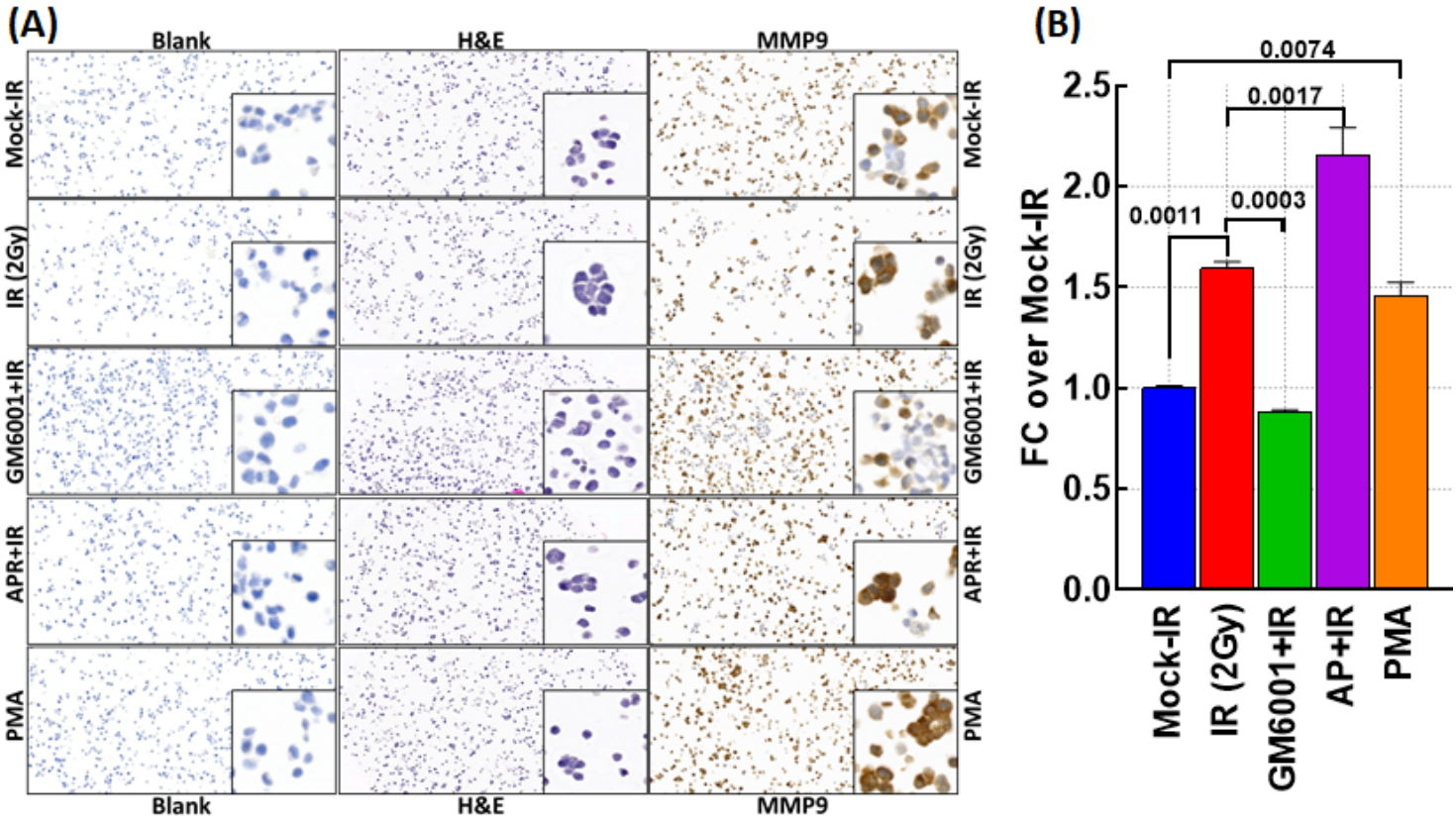

Figure 3

(A) Representative IHC microphotographs from the custom archived cell microarray (CMA) showing MMP9 expression in IMR-32 cells exposed to mock-IR, RT (2Gy), PMA, treated with GM6001 and exposed to RT or, treated with aprotinin and exposed to RT. No antibody IgG controls (blank) and H&E staining are included for each condition. Images are at 10x and the inserts are at 40x magnification. (B) Histograms from the aperio spectrum image analysis quantification of the digitally scanned virtual images showing MMP9 expression in IMR-32 cells exposed to mock-IR or RT with/without MMP9 inhibition. Expression (mean and SEM) is graphed as fold change over mock-IR control. Group wise comparisons are made with ANOVA with Tukey's post-hoc comparison. A P value of ≤ 0.05 is considered significant.

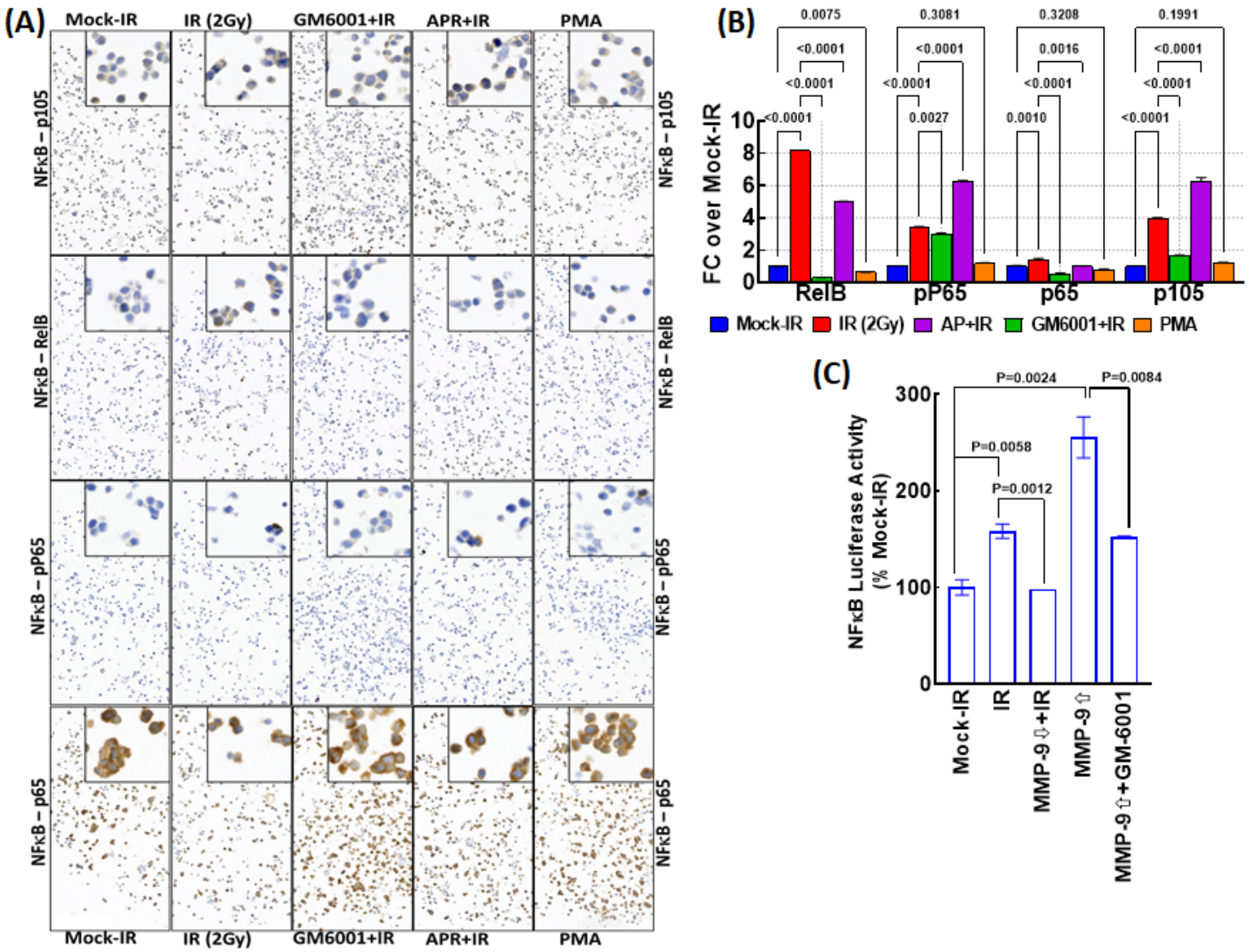

Figure 4

(A) Representative IHC microphotographs from the custom archived CMA showing NFkB-p105, NFkB-RelB, NFkB-p65 expression and NFkB-p65 phosphorylation in IMR-32 cells exposed to mock-IR, PMA, RT with and without GM6001 or aprotinin treatment. Images are at 10x and the inserts are at 40x magnification. (B) Histograms from the aperio spectrum image analysis quantification of the digitally scanned virtual images showing NFkB-p105, NFkB-RelB, NFkB-p65 expression and NFkB-p65 phosphorylation in IMR-32 cells exposed to mock-IR or RT with/without MMP9 inhibition. Expression (mean and SEM) is graphed as fold change over mock-IR control. Group wise comparisons are made with two-way ANOVA with Tukey's post-hoc comparison. A P value of ≤ 0.05 is considered significant. (C) Luciferase assay showing MMP9 dependent NFkB transcriptional activity. SH-SY5Y cells exposed to mock-IR, RT with/without GM6001 treatment, RT with/without shRNA mediated MMP9 silencing or in cells with ectopic expression of MMP9 were transfected with pNFkB-Luc. Data shown represent mean and SEM of three independent experiments.

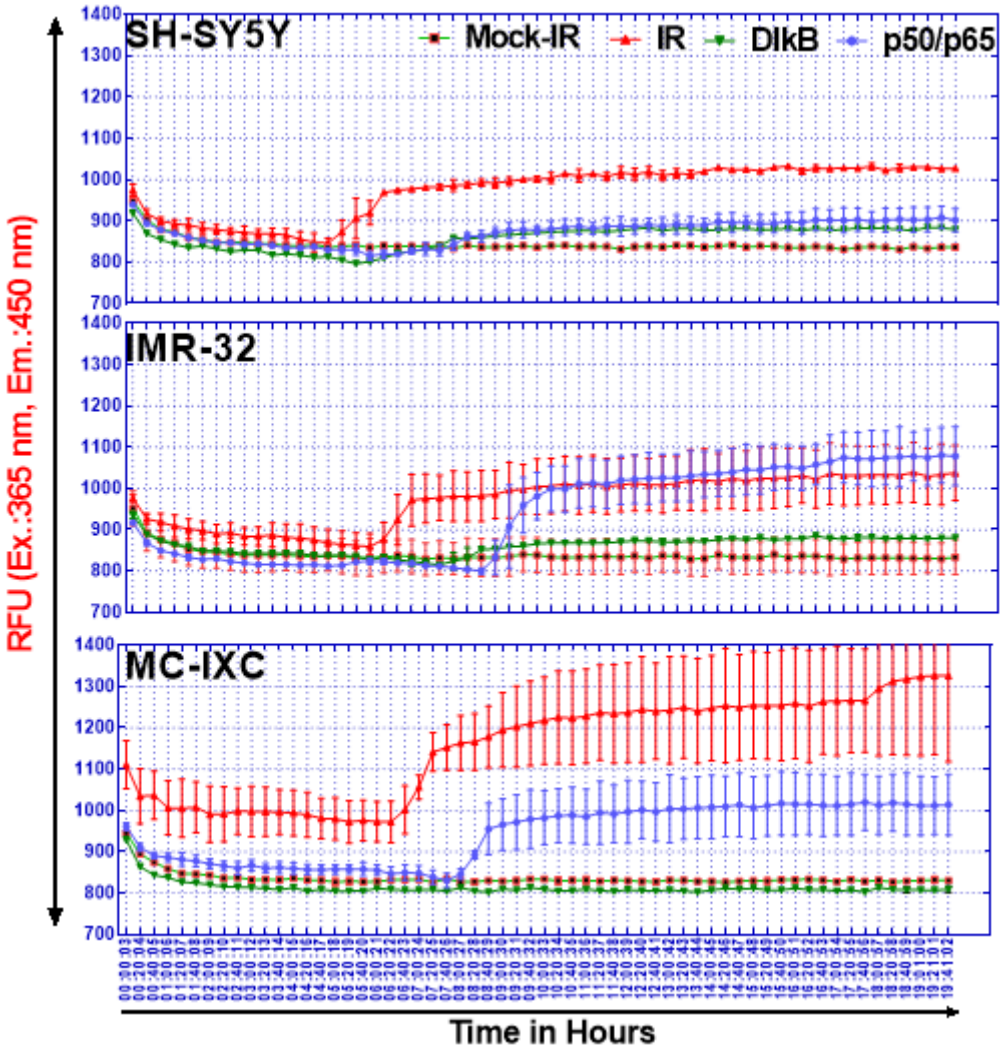

Figure 5

Line graphs obtained from fluorogenic substrate specific activity assay showing MMP9 activity kinetics in the conditioned medium of NB cells (SH-SY5Y, IMR-32 and MC-IXC) exposed to mock-IR, RT, NFkB inhibition with s32A/s36A double mutant IkBα (ΔIkBα) and exposed to RT, or after NFkB (NFkB-p50/p65) overexpression. Kinetics of the MMP9 activity was quantified continuously for every each 20minutes constantly for 20h.

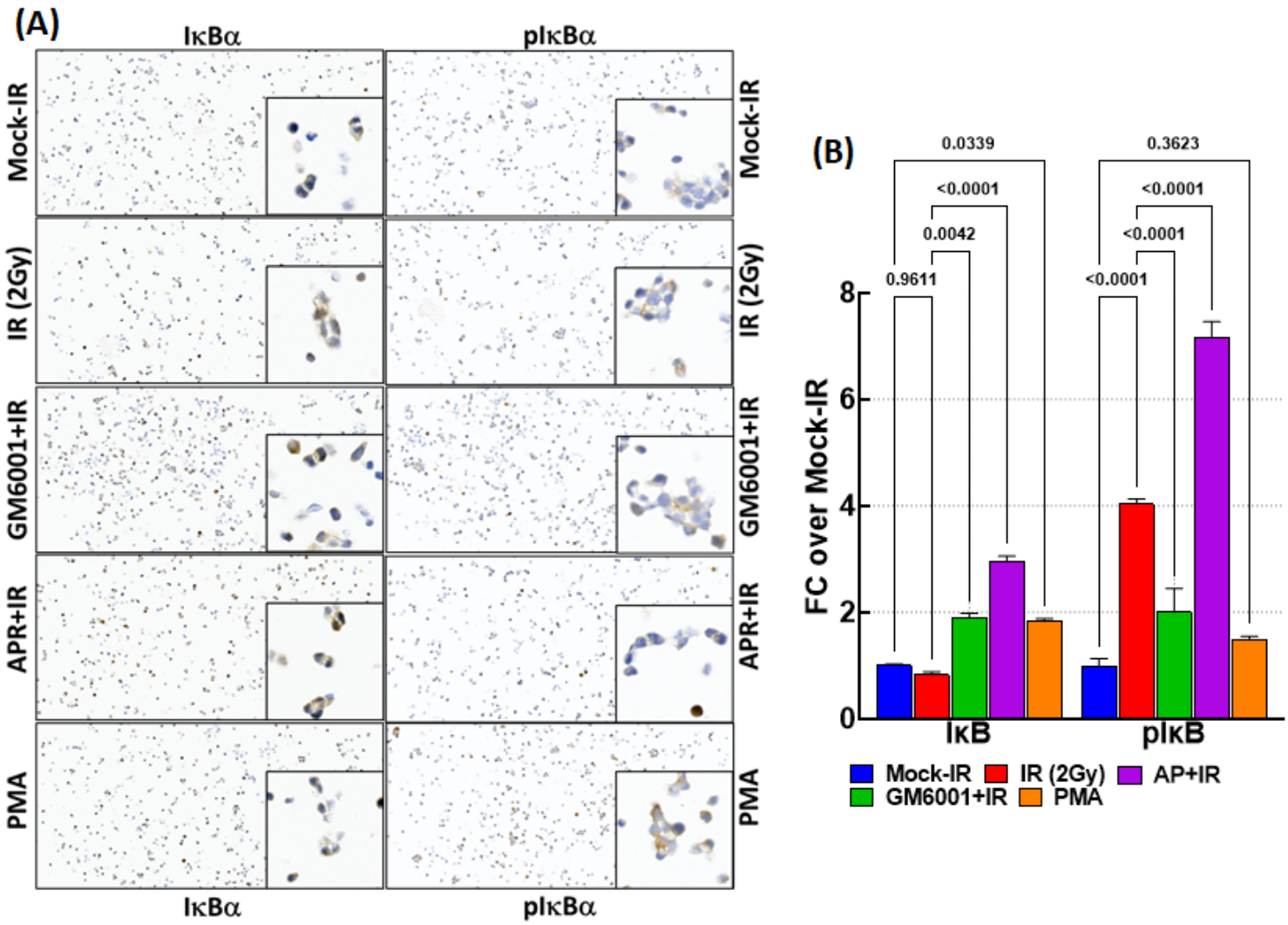

Figure 6

(A) Representative IHC microphotographs from the custom archived CMA showing I□Bα expression and phosphorylation in IMR-32 cells exposed to mock-IR, PMA, and RT with and without GM6001 or aprotinin treatment. Images are at 10x and the inserts are at 40x magnification. (B) Histograms from the Aperio spectrum image analysis quantification of the digitally scanned virtual images showing I□Bα expression and phosphorylation in IMR-32 cells exposed to mock-IR or RT, with/without MMP9 inhibition. Expression (mean and SEM) is graphed as fold change over mock-IR control. Groupwise comparisons were made with two-way ANOVA with Tukey's post-hoc comparison. A P value of 0.05 was considered significant.

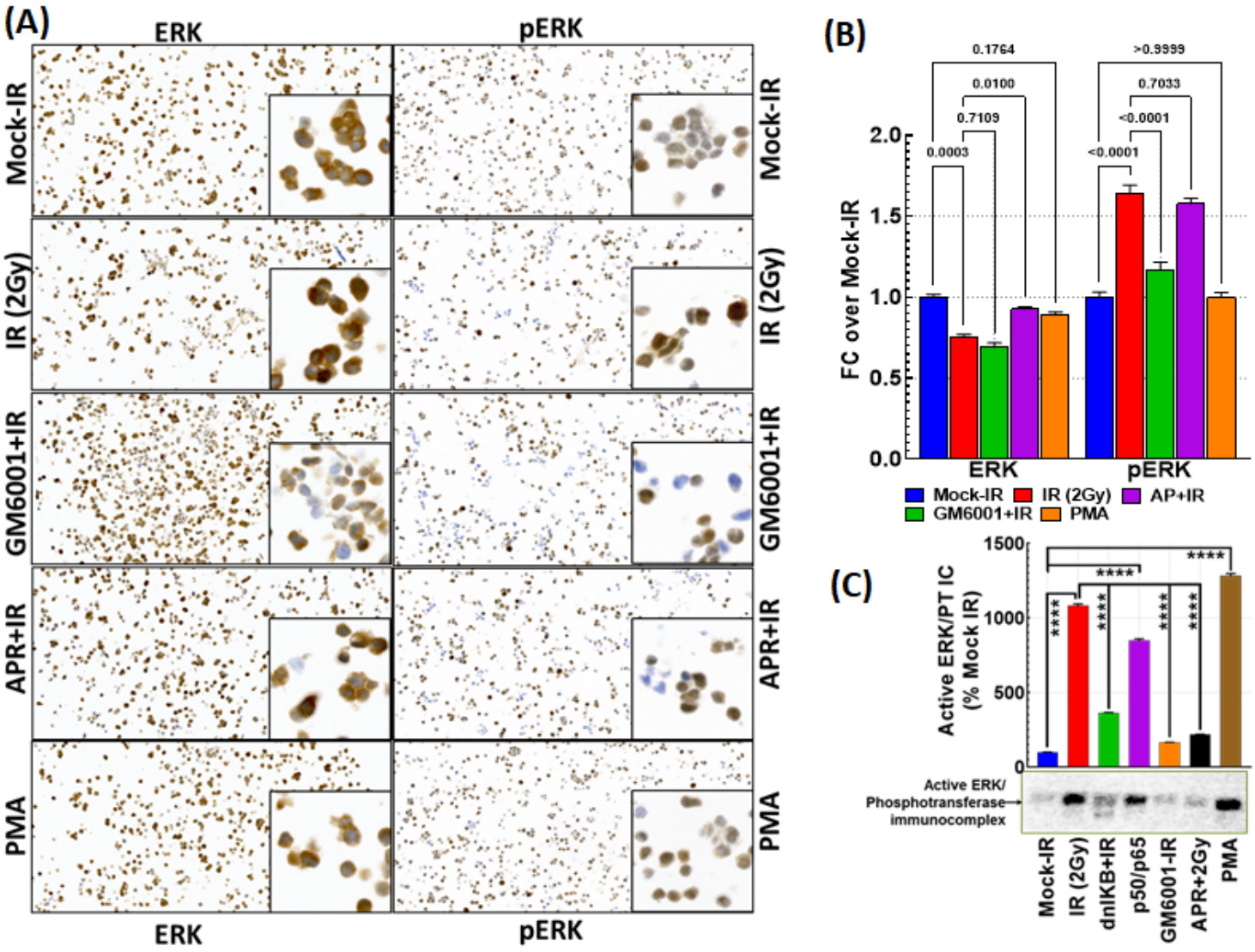

Figure 7

(A) Representative IHC microphotographs from the custom archived CMA showing ERK expression and phosphorylation in IMR-32 cells exposed to mock-IR, PMA, RT with and without GM6001, or aprotinin treatment. Images are at 10x and the inserts are at 40x magnification. (B) Histograms from the Aperio spectrum image analysis quantification of the digitally scanned virtual images showing ERK expression and phosphorylation in IMR-32 cells exposed to mock-IR or RT with/without MMP9 inhibition. Expression (mean and SEM) is graphed as fold change over mock-IR control. Groupwise comparisons were made with two-way ANOVA with Tukey's post-hoc comparison. A P value of 0.05 was considered significant. (C) MMP9-dependent ERK phosphotransferase activity. Representative immunoblot from MAP Kinase/ERK Kinase assay showing alterations in ERK phosphotransferase activity in SH-SY5Y cells exposed to mock-IR, RT, PMA, NF□B inhibition with s32A/s36A double mutant I□Bα (ΔI□Bα) and exposed to RT, treated with GM6001 and exposed to RT, treated with aprotinin and exposed to RT, or after NF□B (NF□B-p50/p65) overexpression. Histograms obtained from 1D gel analysis of immunoblot showing altered levels of ERK phosphotransferase activity. Groupwise comparisons were made with ANOVA with Tukey's post-hoc comparison. A P value of ≤ 0.05 was considered significant.

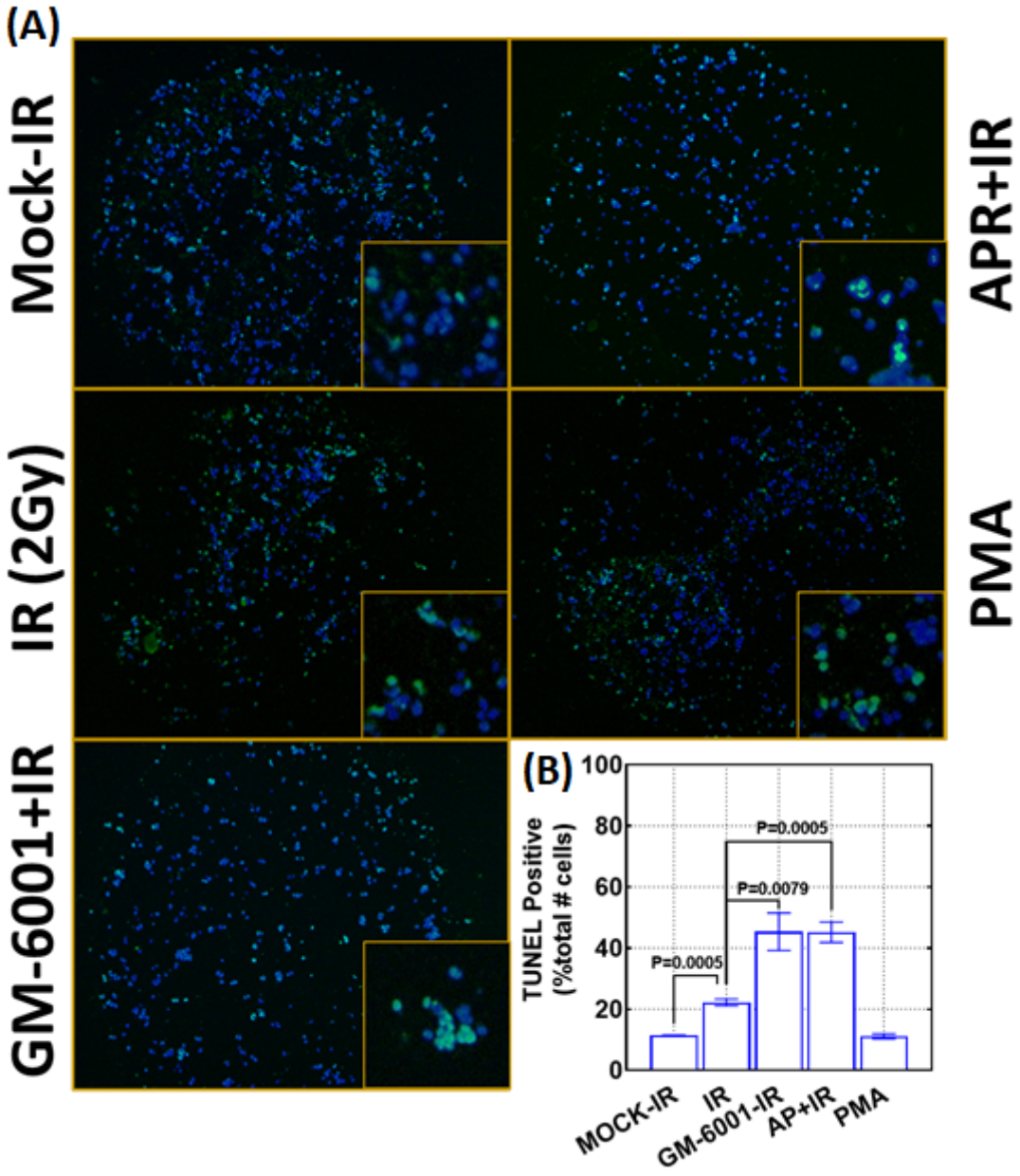

Figure 8

(A) Microphotographs of TUNEL assay showing apoptotic cell death in IMR-32 cells exposed to mock-RT, PMA, RT with and without GM6001 or aprotinin treatment. Images are at 10x and the inserts are at 40x magnification. (B) Histograms from NIH ImageJ analysis quantification showing variations in cell death. Number of apoptotic cells normalized to total number of cells were computed and the mean and SEM were plotted. Groupwise comparison were performed using ANOVA with Tukey's post-hoc correction.

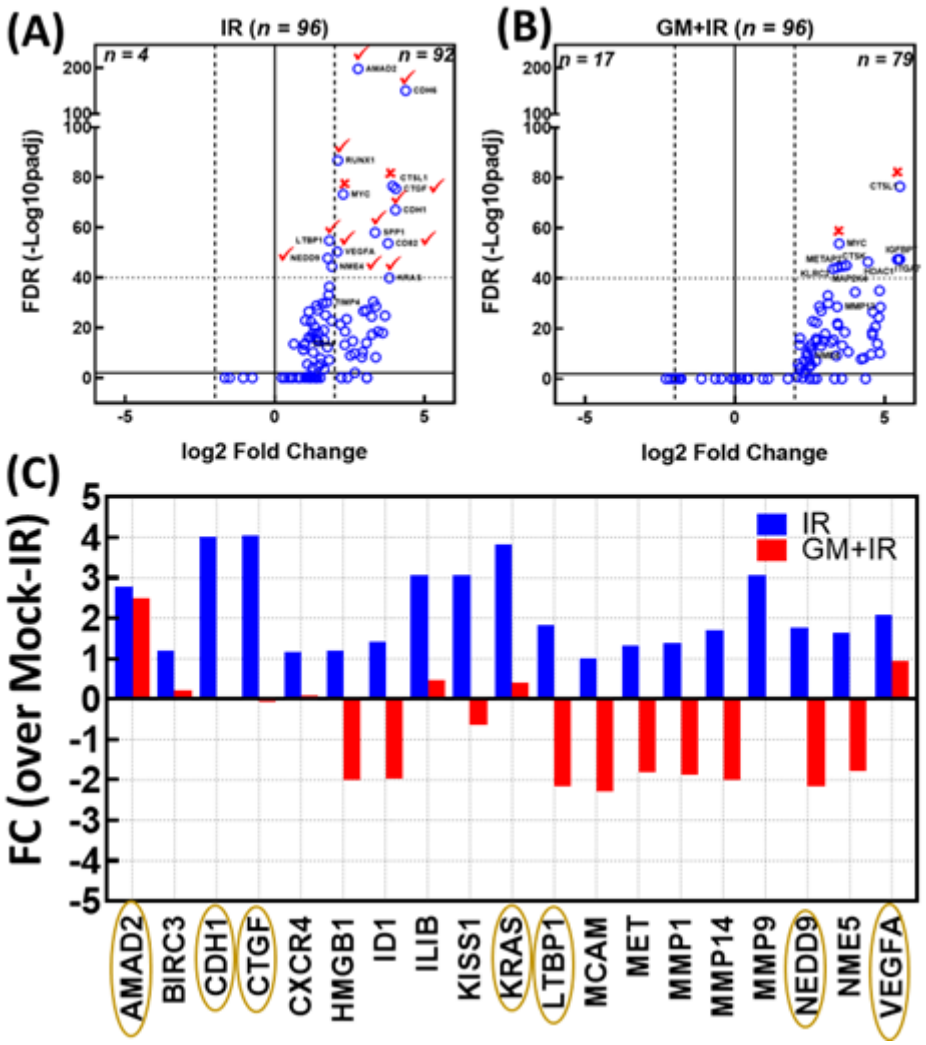

Figure 9

Volcano plots from custom archived QPCR profiling of 93 genes pertaining to tumor invasion and metastasis signaling showing genes modulated (up/down) genes in SH-SY5Y cells (A) exposed to RT (2Gy) and (B) treated with GM6001 and exposed to RT. The ΔΔct values were calculated by normalizing the gene expression levels to positive controls (β-actin, GAPDH, Hprt1), compared between groups, and the relative expression level of each gene was expressed as a fold change. Differential gene expression analysis with stringent criteria (log2 fold change) coupled with false discovery rate calculation were used identify the genes altered with RT with/without inhibition of RT-activated MMP9. (C) Histograms showing significant downregulation of 19 RT-upregulated genes with the inhibition of RT-induced MMP9.

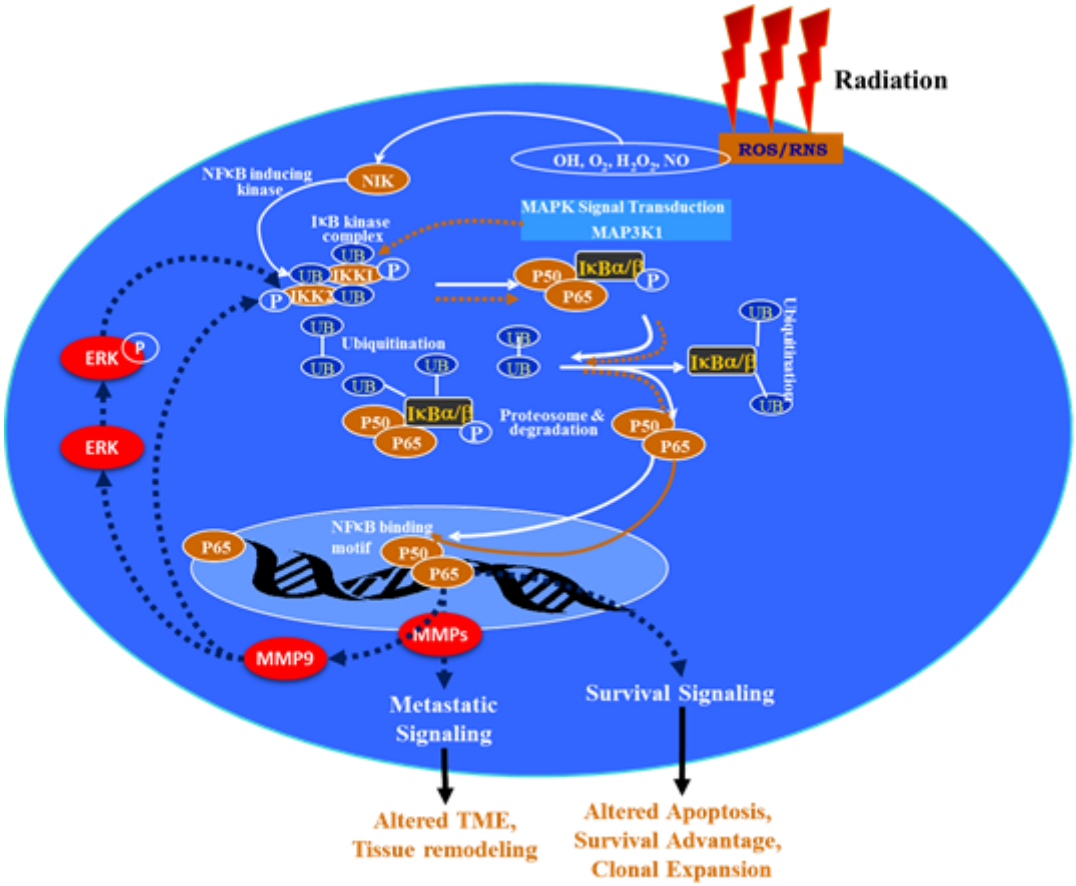

Figure 10

Schematic representation of therapy pressure-related rearranged signaling in NB cells. RT-triggered NF□B activates MMP9, which in turn activates ERK and IKKβ. ERK and IKKβ activity-dependent phosphorylation of I□Bα leads to the second phase activation of NF□B. This RT-induced NF□B-triggered NF□B-MMP9-NF□B PFC signaling leads to the maintenance of activated MMP9, which leads to the NF□B-dependent survival advantage and MMP9-dependent tumor growth invasion and metastasis.